Illuminating heavy element production using MeV gamma-rays and metal-poor stars

Nicole Vassh

TRIUMF Theory Group

September 9, 2026

Nuclear Physics in Astrophysics (NPA-XII)

r-process observational anchor 1: Solar abundance peaks

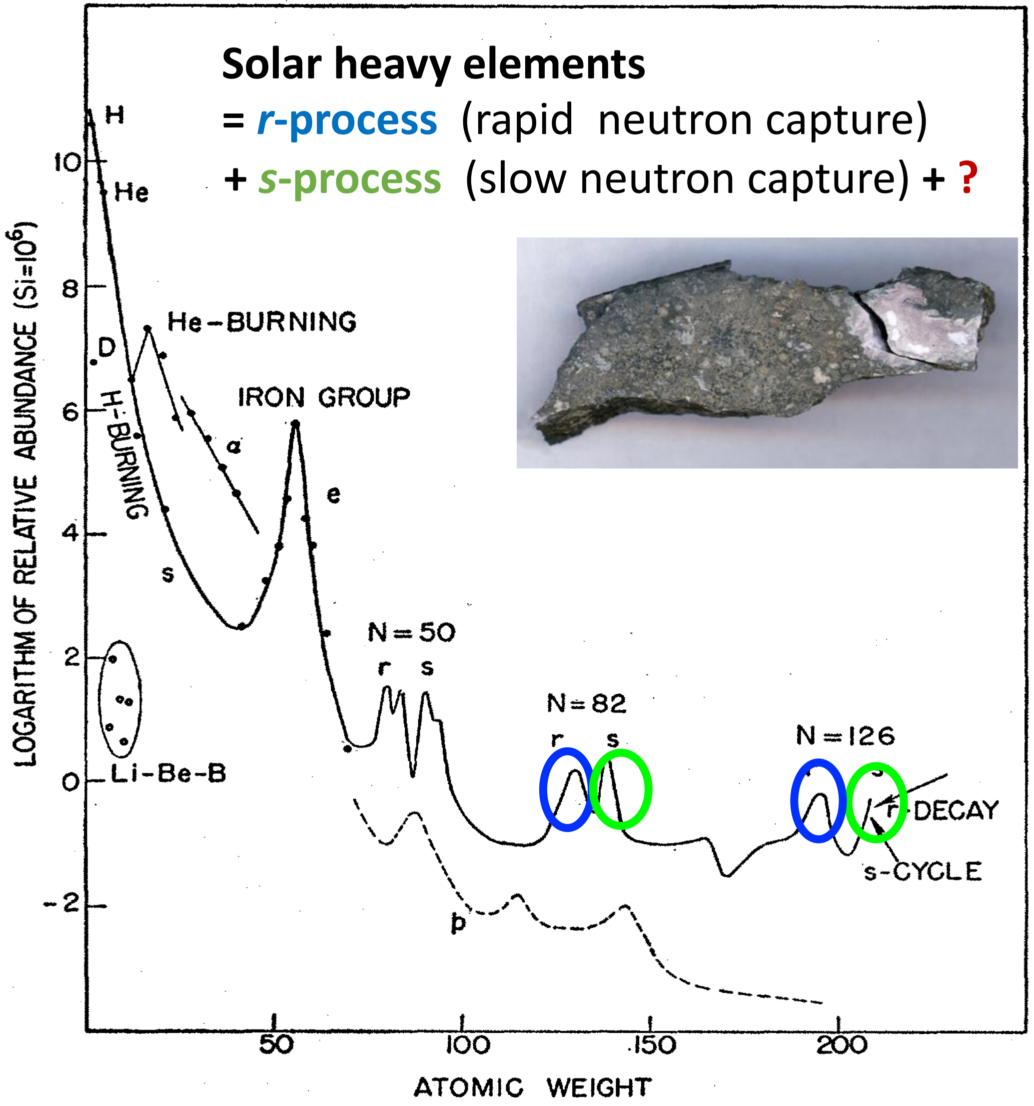

Burbidge, Burbidge, Fowler, and Hoyle (B[2]FH) (1957)

Snapshot @ ~1 sec for very n-rich *r*-process conditions

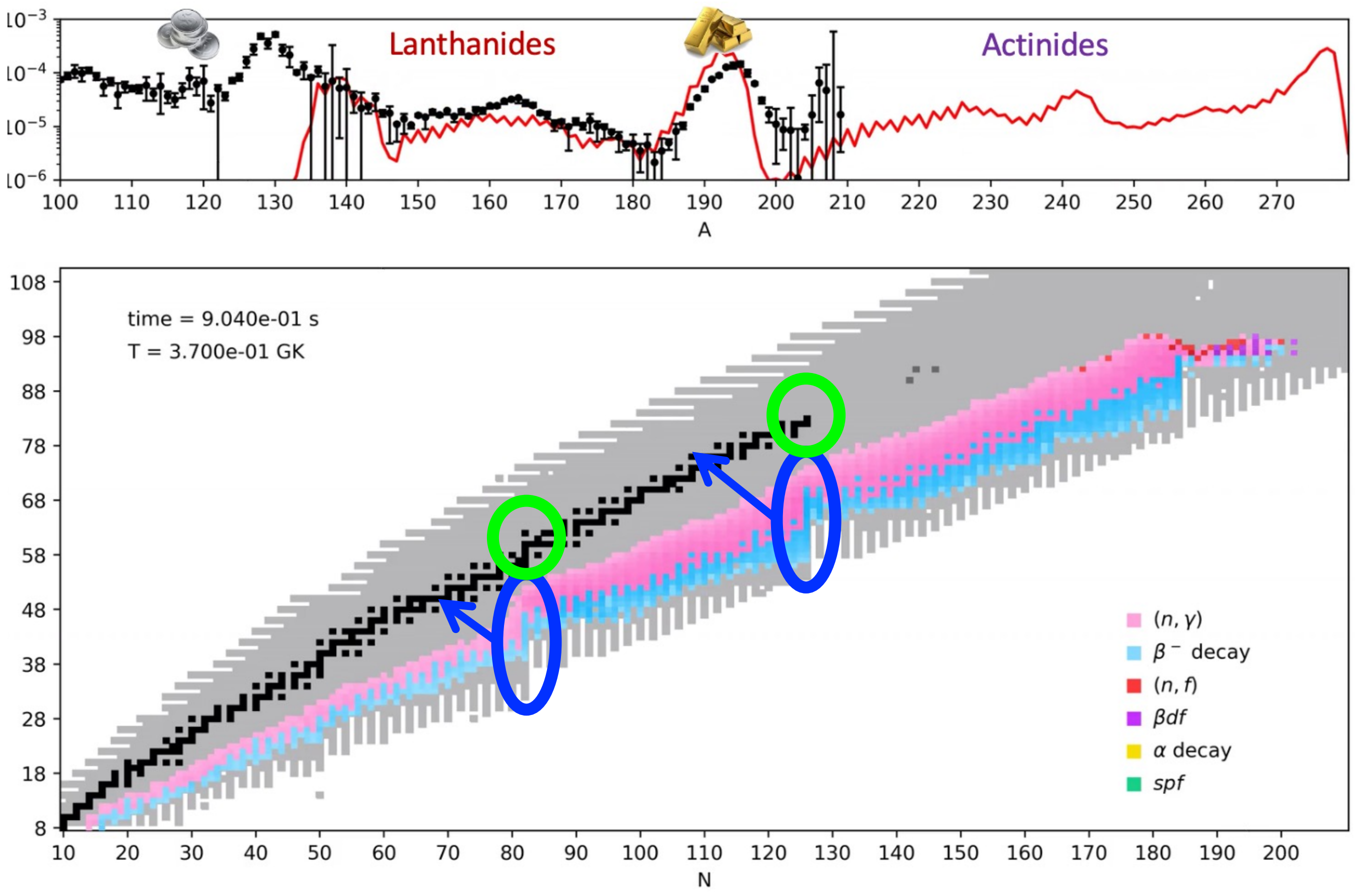

r-process observational anchor 2: metal-poor stars

Metal-poor stars (e.g. low in Fe) likely enriched by one to few events; probe of rare processes such as *r* process

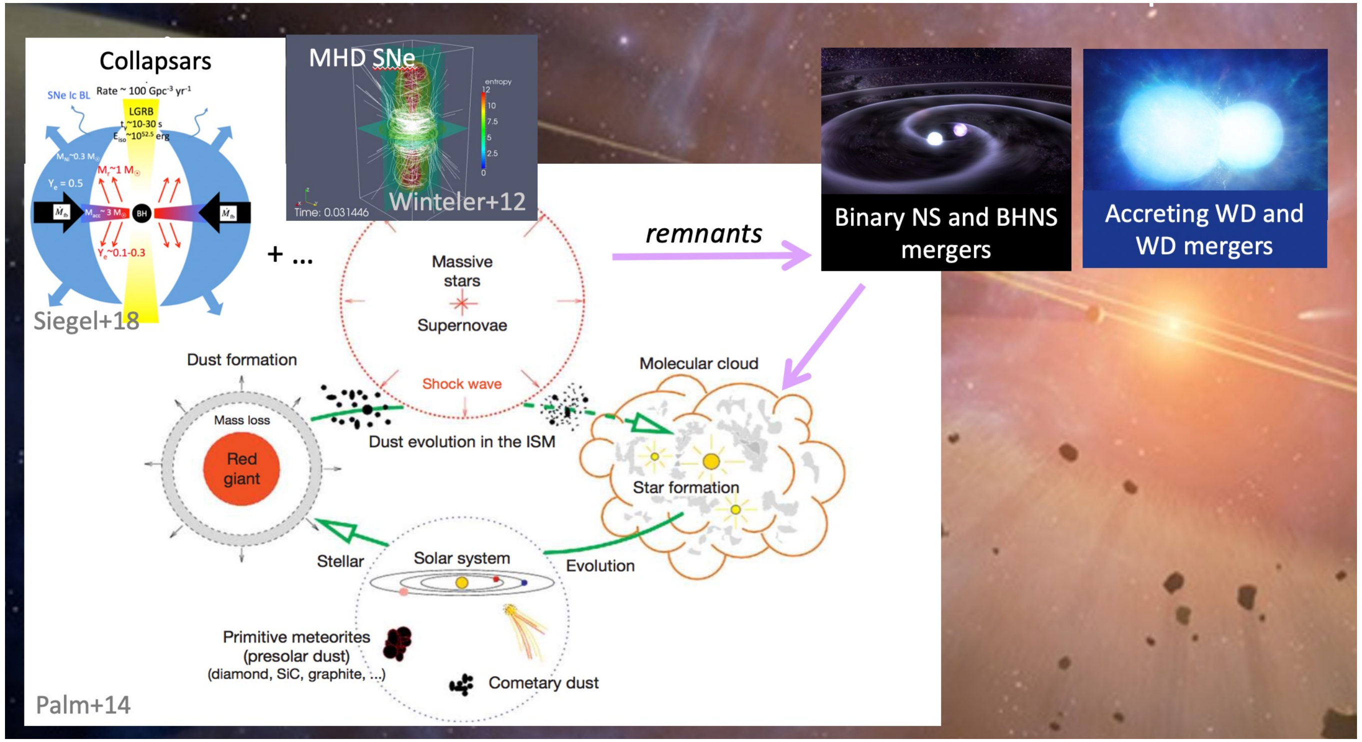

$r - I$: $0.3 \leq$ [Eu/Fe] ≤ 1 and [Ba/Eu] < 0,

$r - II$: [Eu/Fe] > 1 and [Ba/Eu] < 0,

$r - lim$: [Eu/Fe] < 0.3, [Sr/Ba]>0.5, and [Sr/Eu]>0,

s: [Ba/Fe] > 1, [Ba/Eu] > 0.5, and [Ba/Pb]>-1.5.

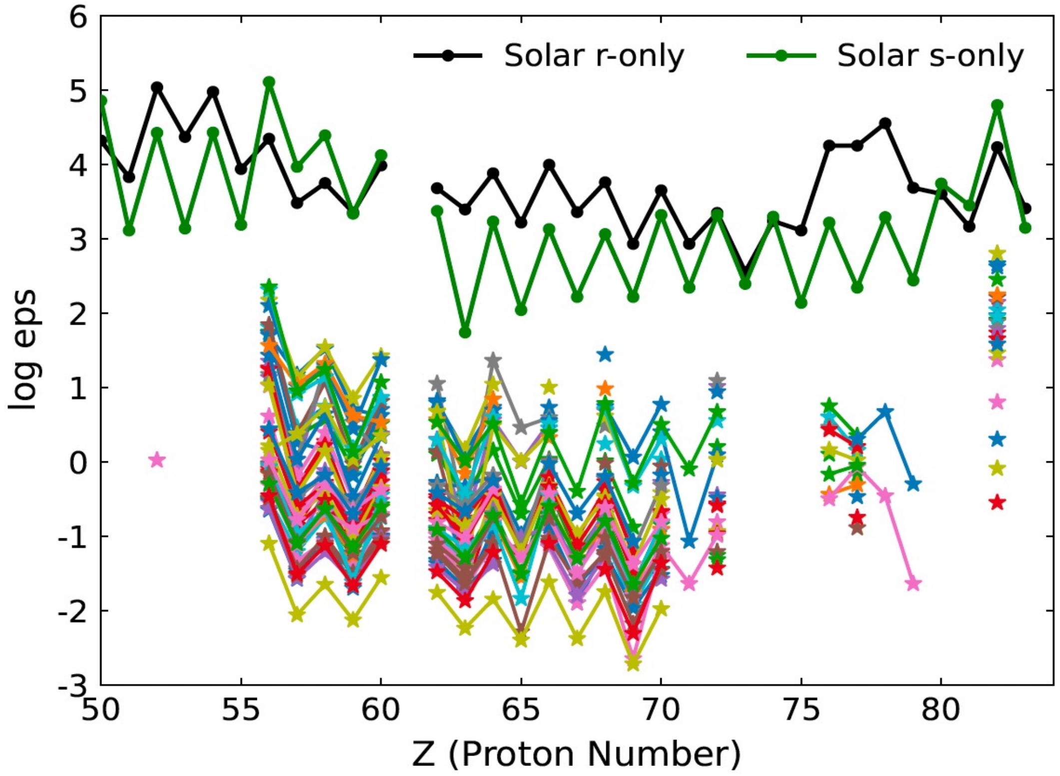

Definitions and stellar data from JINAbase

The nuclear properties of exotic isotopes imprinted in stars

TRIUMF ARIEL
ADVANCED RARE ISOTOPE LABORATORY

Photofission on UC_x target

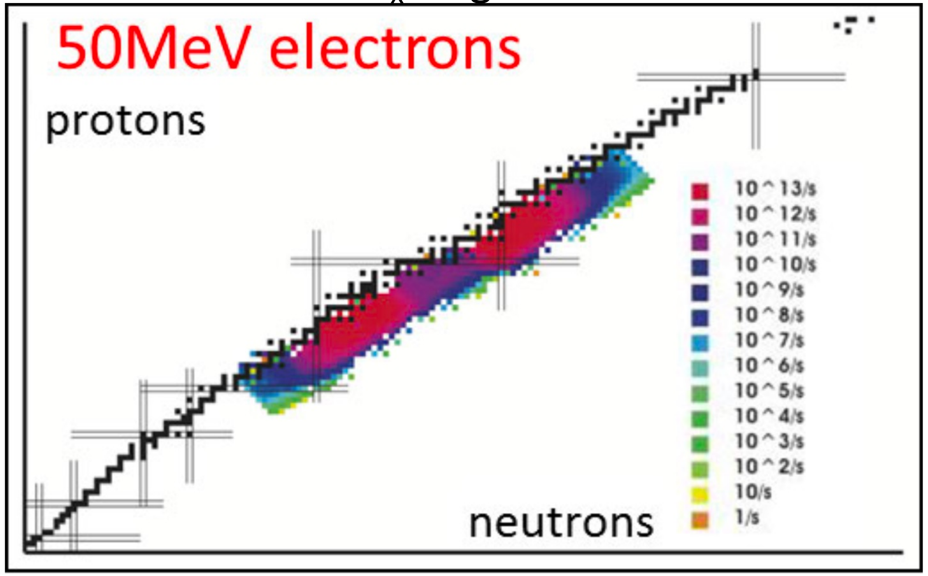

Proton spallation on UC_x target

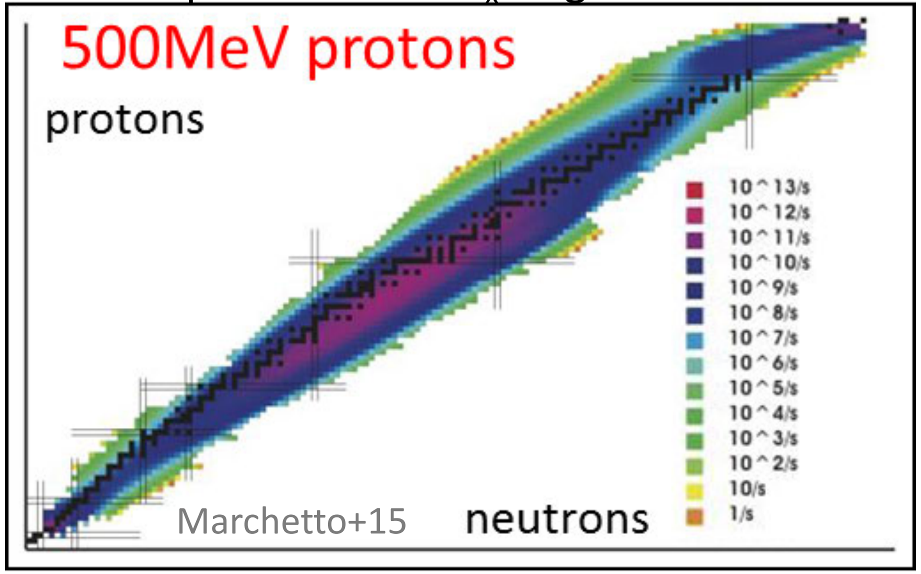

FRIB

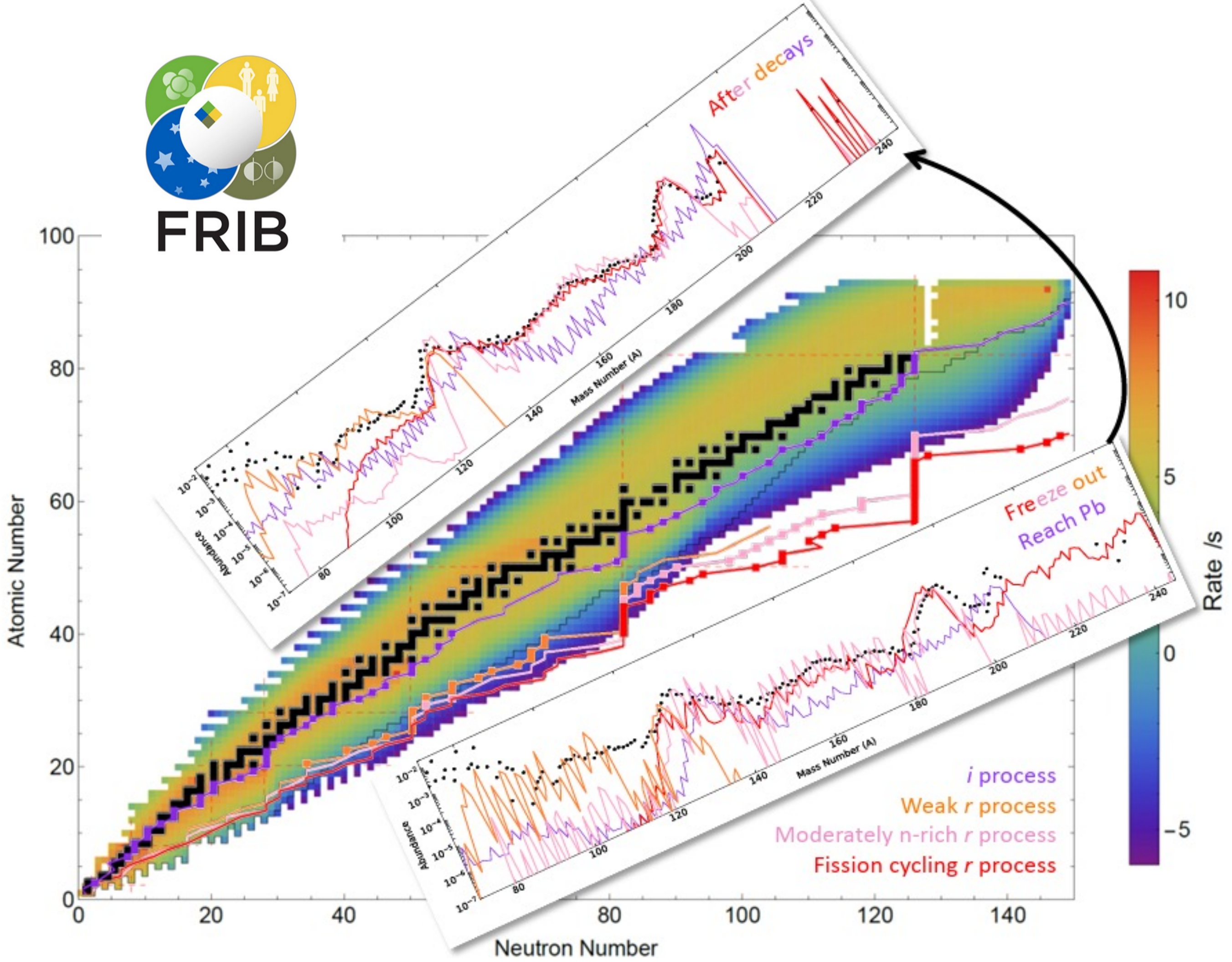

Brown, Gade,…,Vassh, et al. (JPhysG 2025)

r-process observational anchor 3: electromagnetic emission from rare events (e.g. binary neutron star merger *GW170817*)

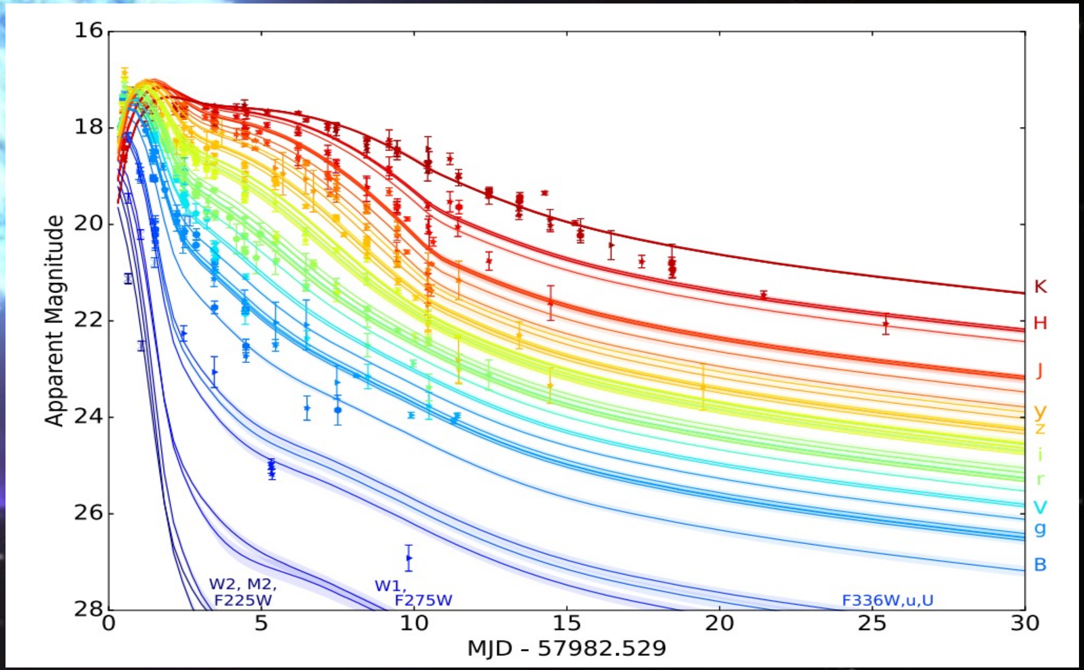

IR

Red bands

Blue bands

Villar+17; see also Cowperthwaite+17

Towards refining calculations of *r*-process observables

Solar system abundances as observed in meteorites

Metal-poor star abundances

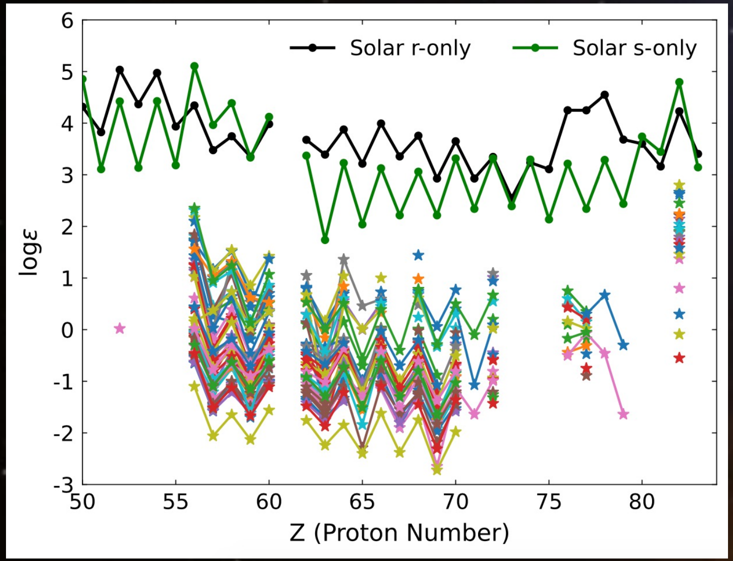

EM emission from rare events

Telescope Campaigns

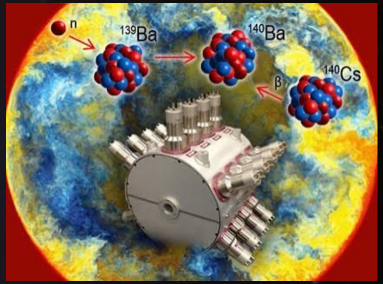

Nuclear Experiment

Machine Learning

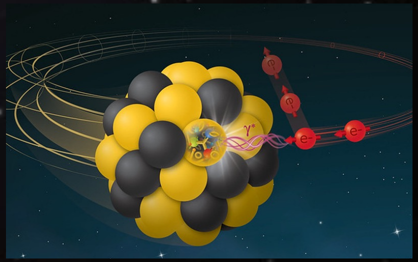

Nuclear Theory

Towards refining calculations of *r*-process observables

Solar system abundances
as observed in meteorites

Metal-poor star abundances

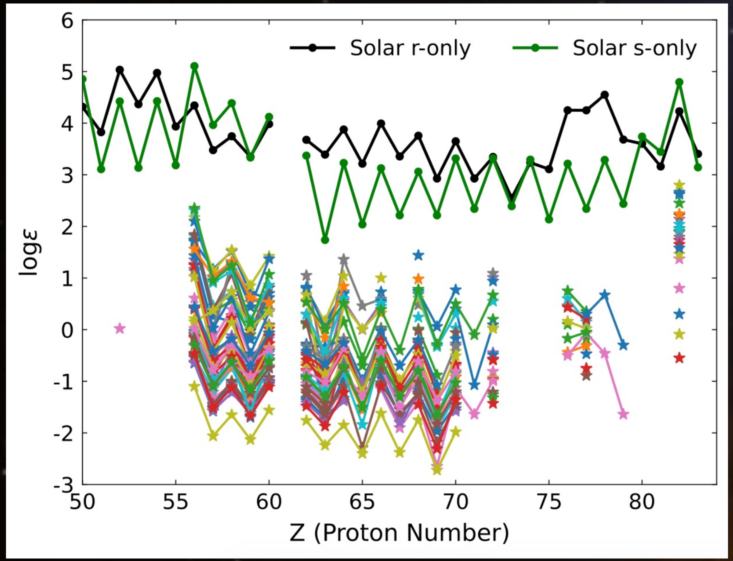

EM emission from
rare events

Telescope
Campaigns

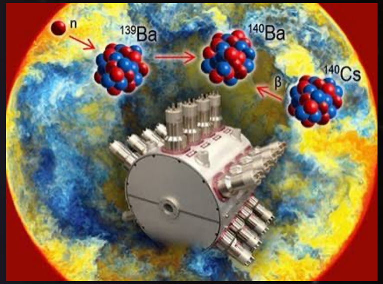

Nuclear
Experiment

Machine
Learning

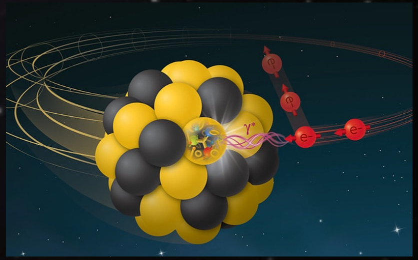

Nuclear
Theory

MeV gamma rays as fingerprints of astrophysical isotope production

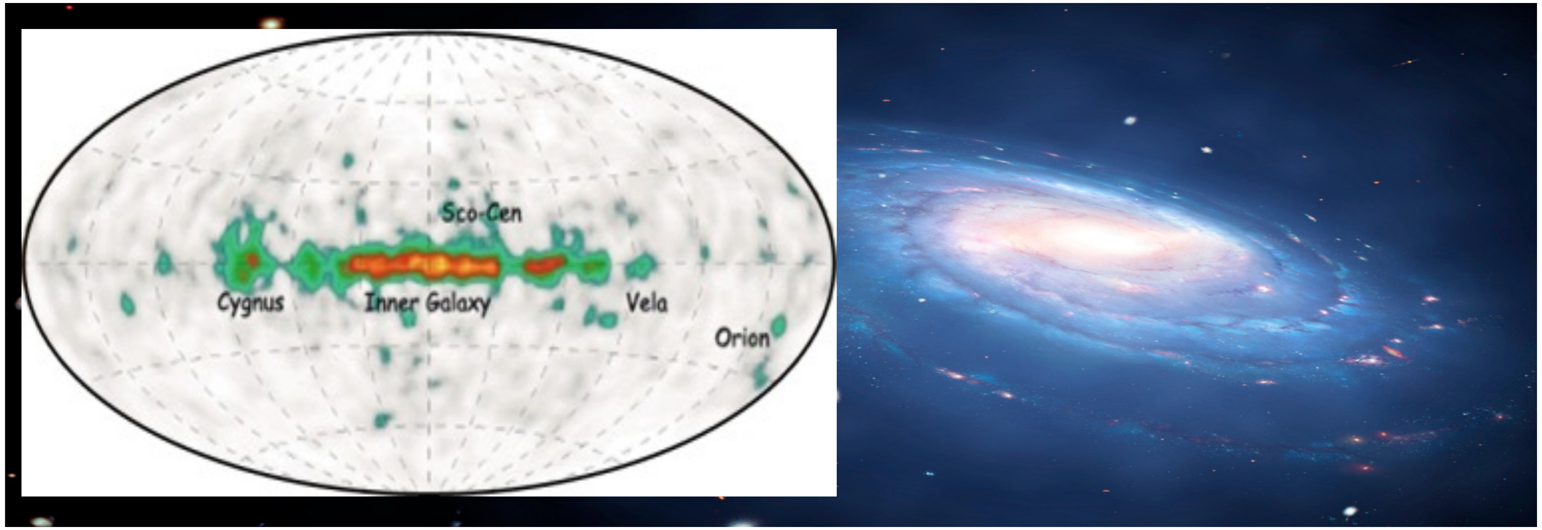

COMPTEL all-sky image of 26Al 1.8 MeV emission from Galactic disk

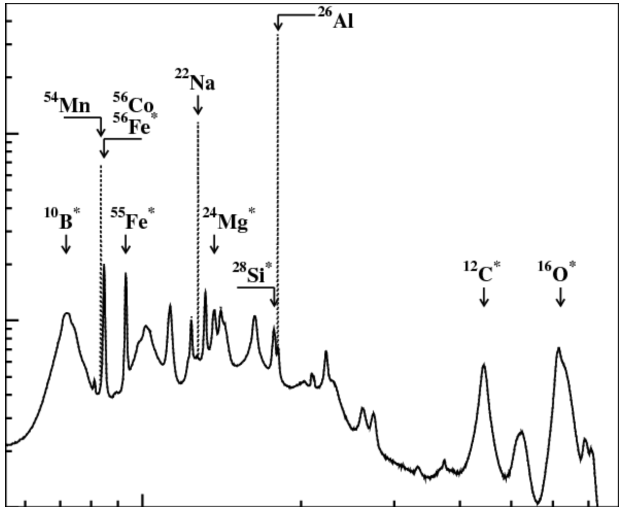

Emission from NSM remnants

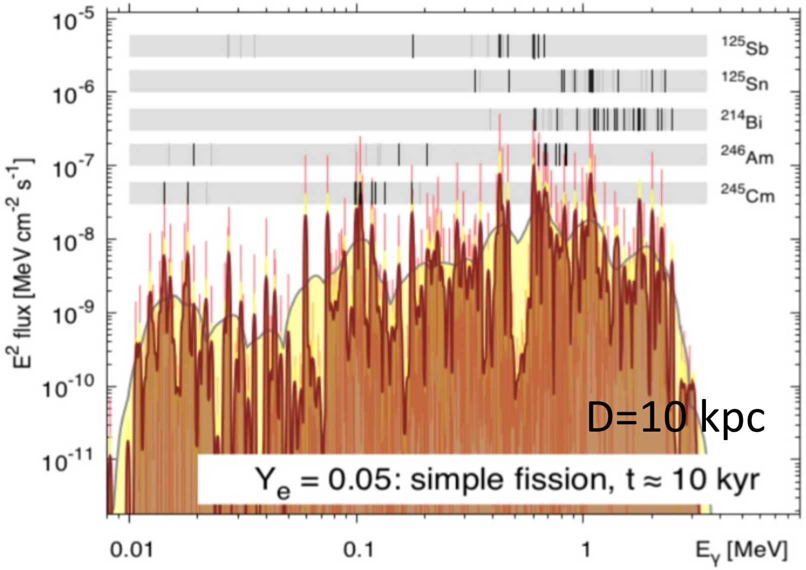

Korobkin+19; see also Wu+19

Emission from a nearby mergers

3day, 3Mpc, 0.01Msun

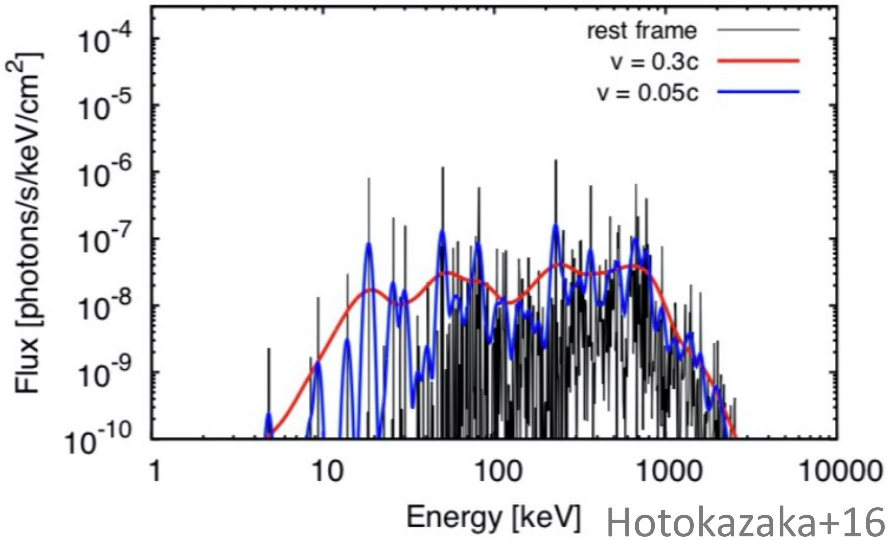

Hotokazaka+16

Predictions for observable MeV gamma emission from fission and the decays of neutron-rich nuclei in mergers

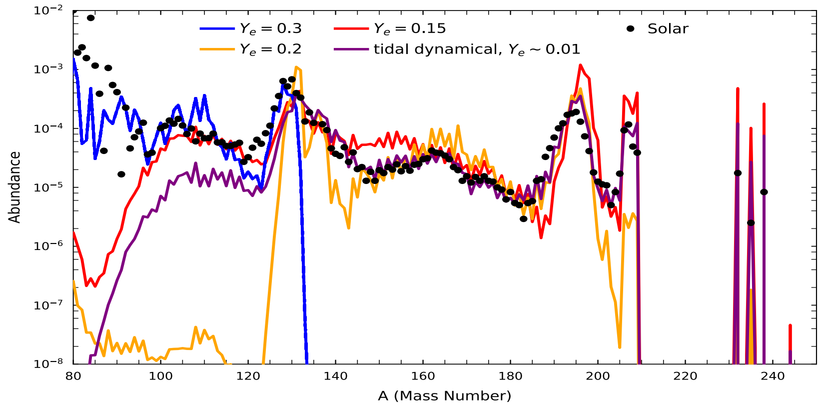

Spectrum with significant emission >3.5 MeV signifies that an astrophysical event produced fissioning species

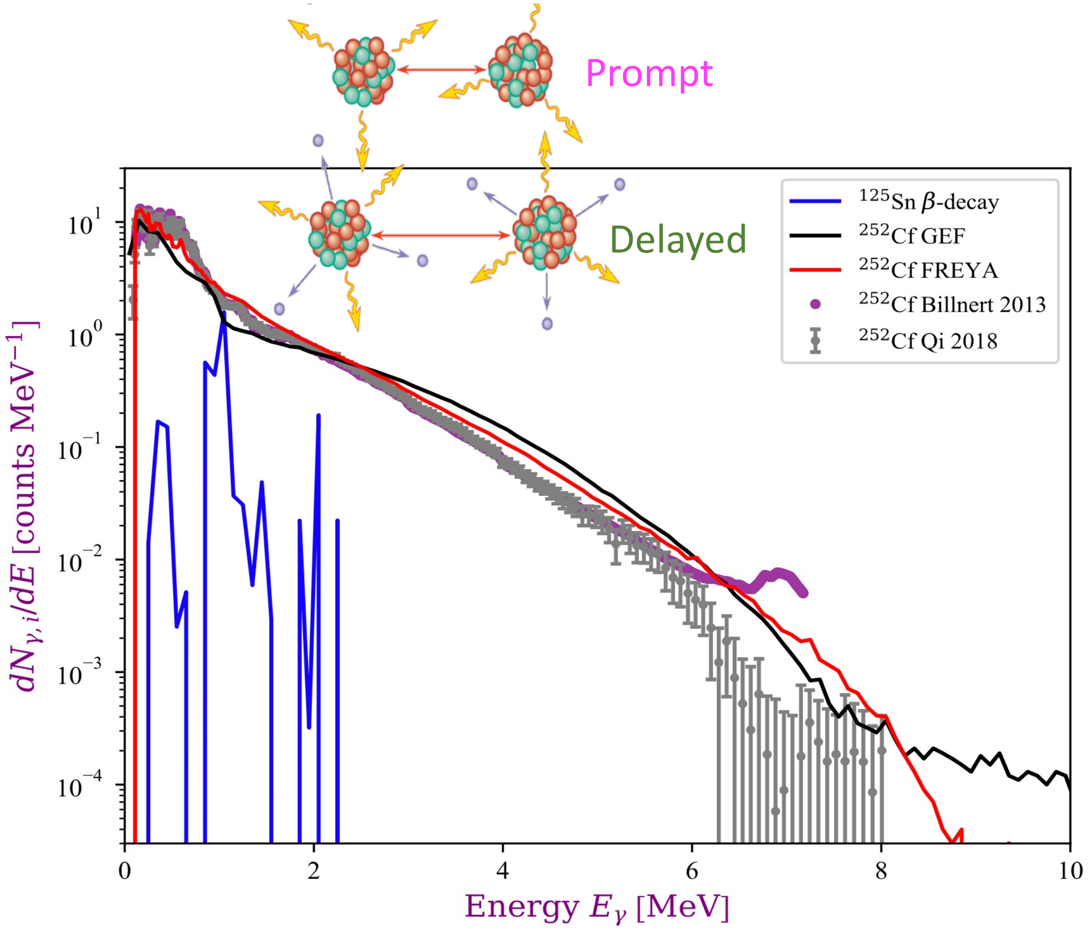

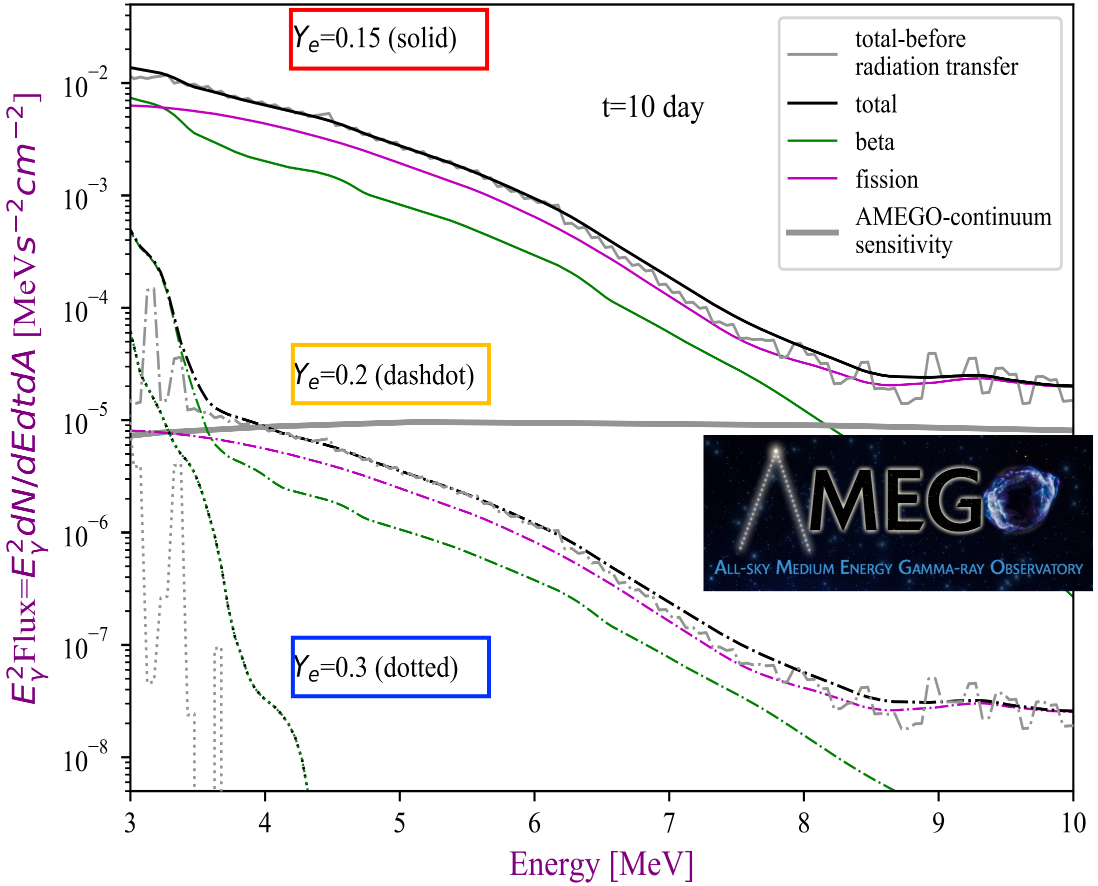

Wang,Vassh+20 (ApJ Letters 903, L3)

The 2.6 MeV gamma-ray line from Tl-208 β-decay: a beacon for numerous disciplines and astrophysics

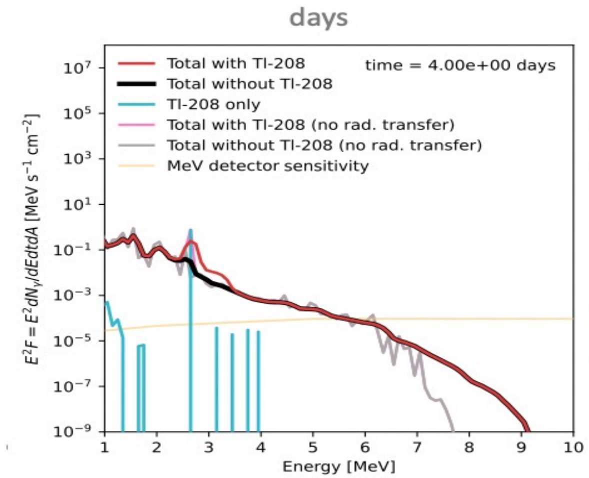

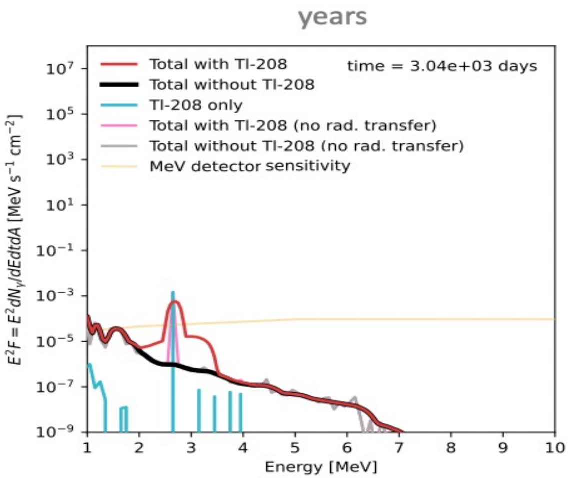

@ 10 kpc (Galactic)

Vassh, Wang+24
(PRL 132, 052701)

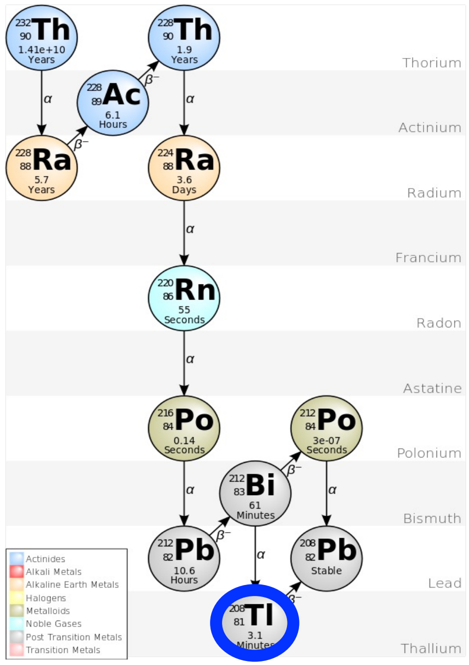

Majorana demonstrator

(^{76}Ge neutrinoless double β-decay search)

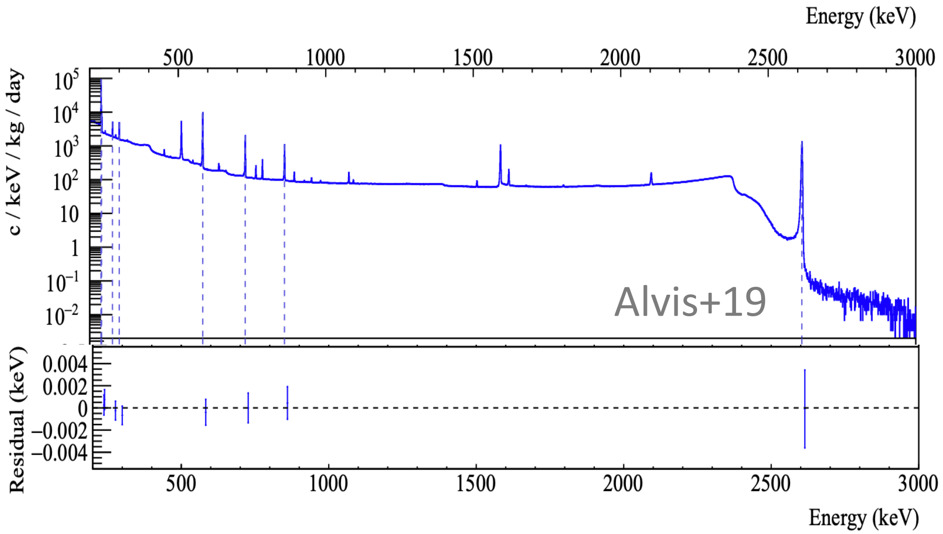

The 2.6 MeV gamma-ray line from Tl-208 β-decay: a beacon for numerous disciplines and astrophysics

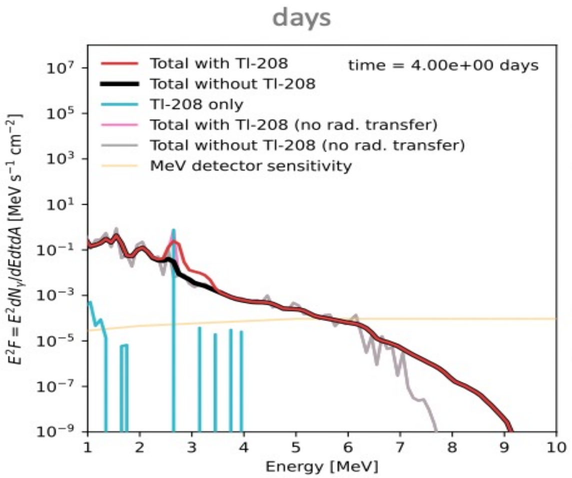

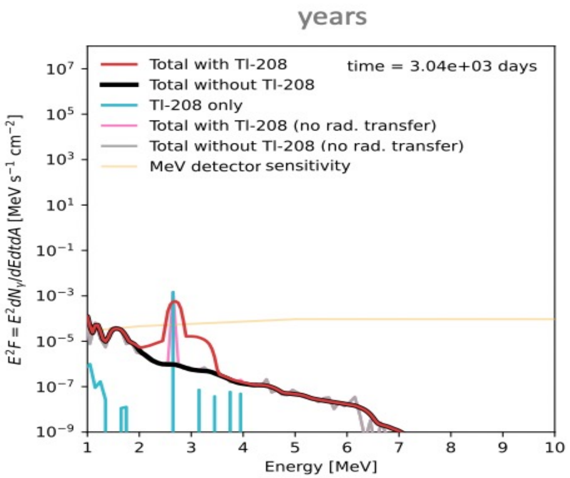

@ 10 kpc (Galactic)

Vassh, Wang+24 (PRL 132, 052701)

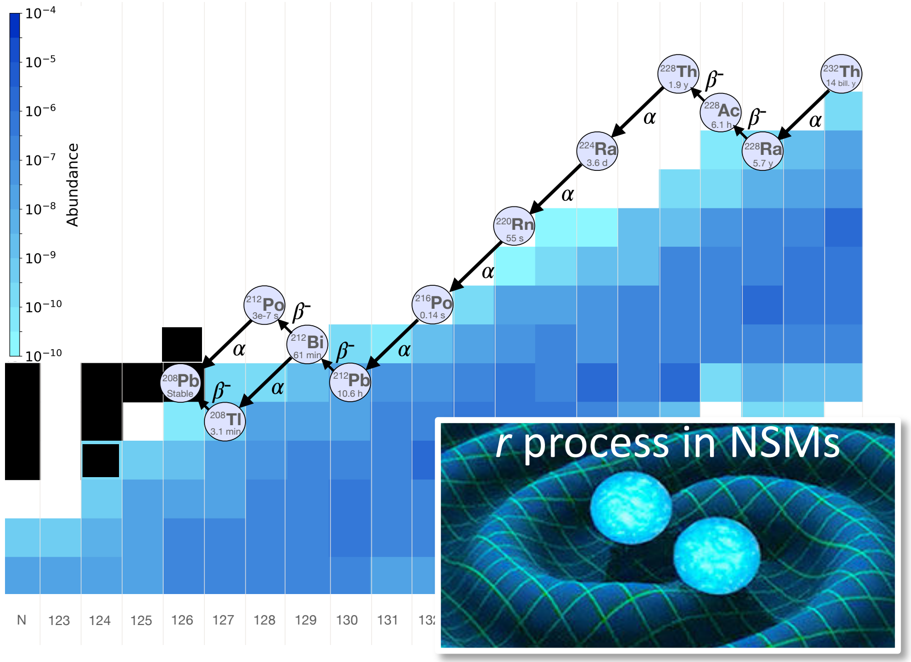

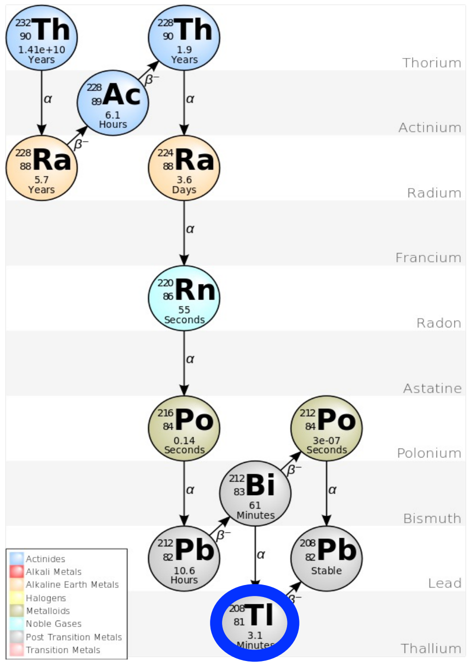

Majorana demonstrator

(^{76}Ge neutrinoless double β-decay search)

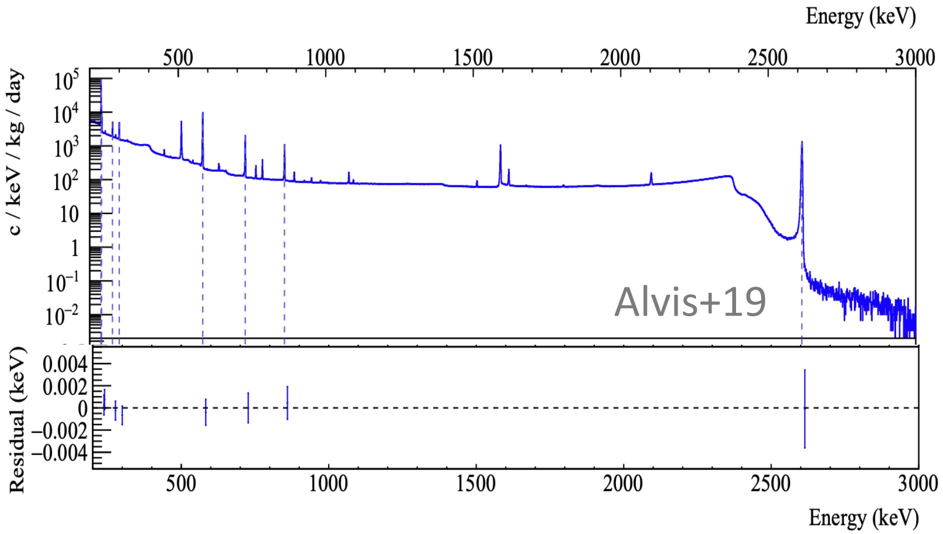

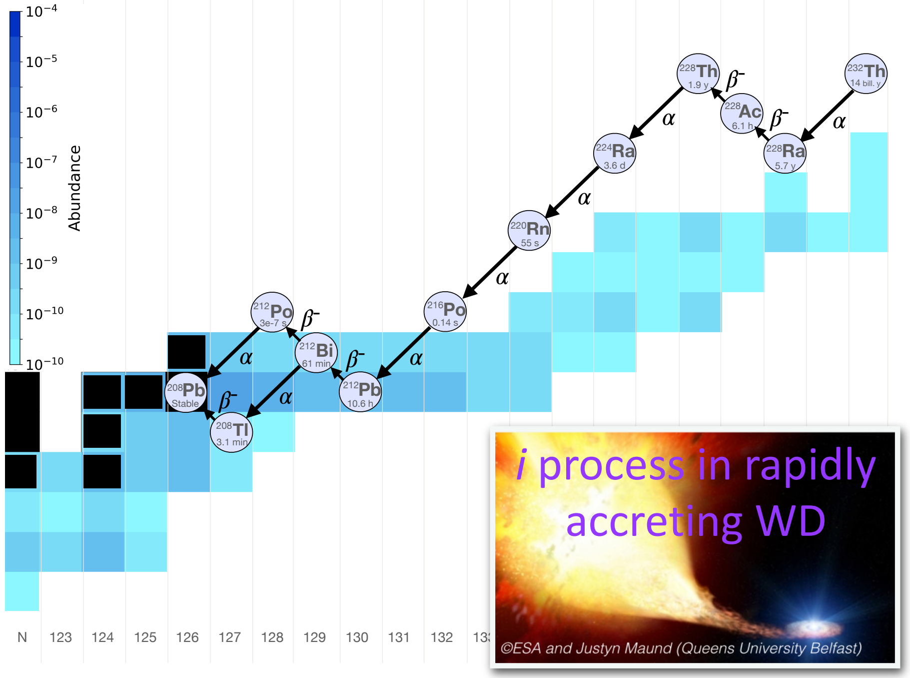

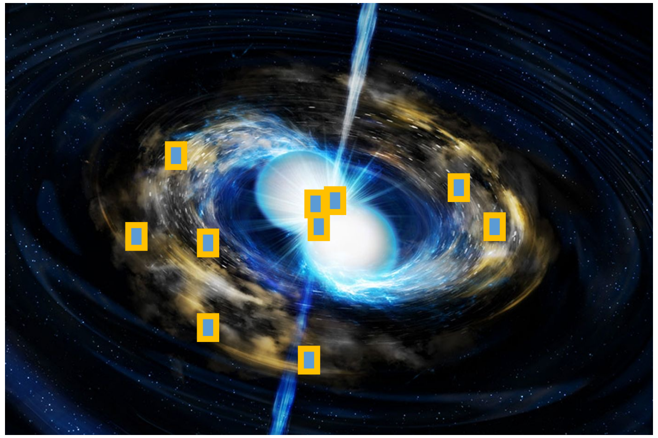

- **Consider a mass weighted sum of merger ejecta** from NSM sim. of Radice et al.
- **Apply a peak finding algorithm** to identify when lines from the decay of specific isotopes may be visible in the total predicted spectrum

UBC/TRIUMF PhD student Maude Lariviere

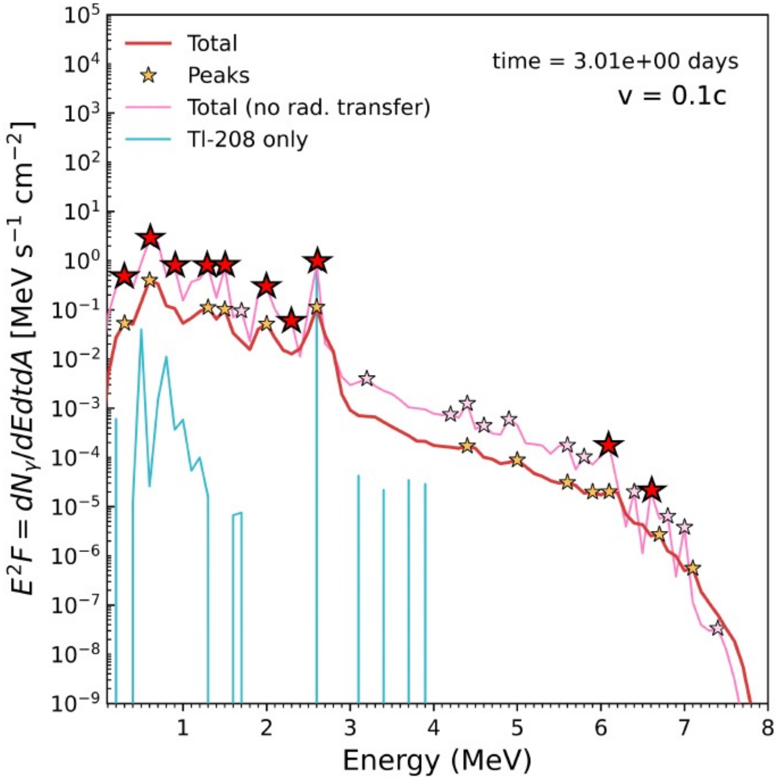

Larivière, Vassh, Deng, Wang, and Surman 26 (submitted, arXiv:2605.17213)

Remnant timescales (>10 years)

Isotope	Time (years)	E (keV)	Mass models	mkt Betas
K-42	7.49e+01 – 1.40e+02	1525	–	F
Co-60	2.65e+03 – 8.41e+06	1173	*	*
	1.02e+03 – 7.93e+06	1332	*	*
Rh-106	8.25e-01 – 1.24e+01	2366	–	T
In-128	3.77e+01 – 3.86e+01	3520	*F*	–
Sb-125	9.16e-01 – 1.32e+01	**428**, 463	T	FT
	1.90 – 1.94e+01	**601**, 636	FT	FT
Sb-126	5.26e+02 – 2.02e+06	415	*	*
	5.70e+01 – 2.18e+06	**666**, 695, 697	*	*
Sb-134	6.27e-01 – 2.20e+02	6451	–	H
	1.00e-03 – 3.84e+01	6687	*H*	H
	1.00e-03 – 1.53e+01	6820	H	H
I-136	1.64e+02 – 2.09e+02	6104	*H*	H
Ir-194	1.22e+01 – 5.45e+01	328	FT	FT
	7.95 – 3.70e+01	939	–	T
	2.87 – 6.31e+01	**1151**, 1183	FT	FT
	2.29 – 5.32e+01	1469	–	FT
	3.94 – 5.67e+01	1622	–	T
	5.50 – 5.70e+01	1806	*FT*	FT
	7.39 – 5.78e+01	2044	–	FT
Tl-208	4.05e-01 – 1.05e+02	2615	*	*
Tl-209	2.08e+02 – 3.61e+04	1567	*	FT
Ac-228	1.71 – 4.57e+01	**911**, 969	FT	F
	3.26 – 4.67e+01	1588	FT	–
Am-246	8.33e+01 – 3.18e+02	154	–	T

Isotopes with decay lines dominating spectrum some time between 1 day to 1 Gyr

Mass weighted total ejecta from Radice et al. NSM hydrosim

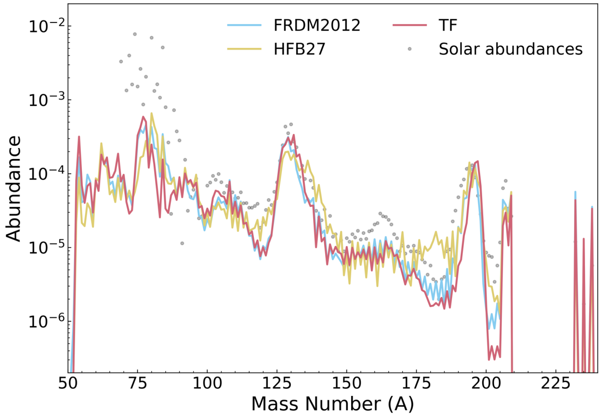

K-42, Fe-59, Co-60, Ga-72, Ge-77, Rb-88, Nb-95, Ru-103, Rh-106, Ag-112, In-128, Sb-125, Sb-126, Sb-128, I-131, I-132, La-140, Pr-144, Eu-156, Ir-194, Tl-208, Tl-209, Ac-228, Am-246

Main *r*-process variations

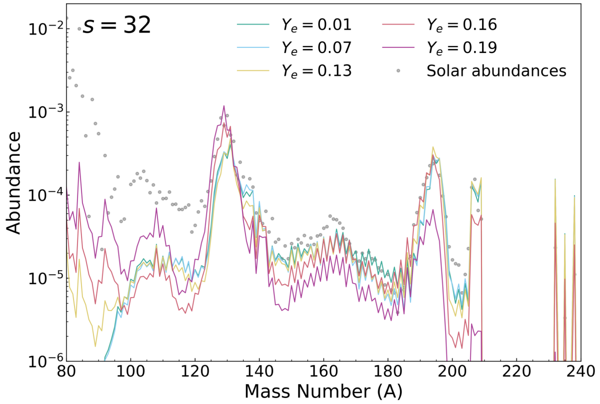

Rb-88, Nb-95, Ru-103, Rh-106, Ag-112, Sn-125, Sn-127, Sb-125, Sb-126, Sb-128, Sb-129, I-131, I-132, I-133, I-135, Xe-133, La-140, La-142, Pr-144, Eu-155, Eu-156, Hf-181, Ta-182, Ta-185, Re-188, Ir-194, Tl-208, Tl-209, Pb-211, Pb-214, Ac-228, Pu-243, Am-246

Weak *r*-process variations

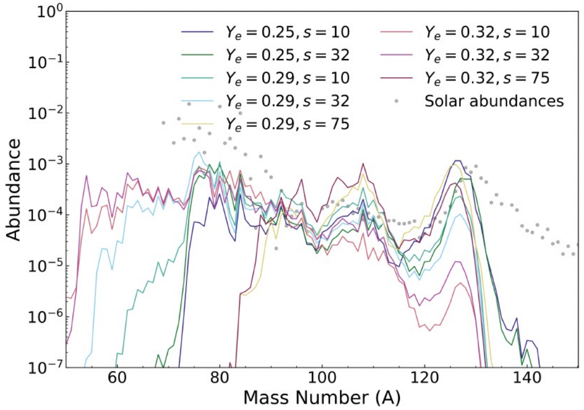

Na-24, K-42, Fe-59, Co-60, Cu-66, Cu-67, Zn-72, Ga-72, Ge-77, Kr-85, Kr-88, Rb-88, Y-91, Zr-95, Nb-95, Ru-103, Rh-106, Ag-112, Sn-125, Sb-125, Sb-126, Sb-127, Sb-128, Sb-129, I-131, I-132, La-140

* Overall, find Fe-59, Co-60, Ga-72, Ge-77, Rb-88, Zr-95, Nb-95, Ru-103, Rh-106, Ag-112, Sn-125, Sb-125, Sb-126, Sb-128, I-131, I-132, La-140, Eu-156, Ir-194, Tl-208, Tl-209, Pb-214, Ac-228 most frequently reported across calculation variations; note appendix also features species with long half-lives that are significantly populated but presently report no strong lines

Larivière, Vassh, Deng, Wang, and Surman 26 (submitted, arXiv:2605.17213)

Smoking guns of solely weak *r*-process production: Ga-72 and Rh-106 spectral takeover

Isotope	Time (days)	E (keV)	Conditions							
			1	2	3	4	5(r)	6(r)	7	8
Ga-72	2.63 – 1.07e+01	630				H		FH	FH	
	1.04 – 1.44e+01	**834**, 894			HT	*		*	*	
	2.98 – 9.22	1051				H				
	2.62 – 1.29e+01	1231, 1260, **1277**			H	*		FH	FH	
	1.56 – 3.07e+01	1464			*	*		*FHT*	*	
	1.14 – 3.12e+01	1597			*	*		*	*	
	1.17 – 3.61e+01	1862		H	*	*		*	*	
	6.44e-01 – 4.16e+01	2202		HT	*	*		*	*	
	4.84e-01 – 4.49e+01	2508	HT	*	*	*		*	*	
	6.84e-01 – 3.54e+01	2844		HT	*	*		*FHT*	*	
	1.12 – 2.21e+01	**3325**, 3339	T	HT	*	*		*FHT*	*	
	7.87e-01 – 1.45e+01	3679		HT	*	*		*	*	

Isotope	Time (years)	E (keV)	Conditions							
			1	2	3	4	5(r)	6(r)	7	8
Rh-106	2.34 – 1.63e+01	873			*	*		*FHT*	*	*
	2.07e-01 – 1.90e+01	1050	*	*	*	*	*	*	*	*
	1.20e-01 – 1.90e+01	1562	*	*	*	*	*	*	*	HT
	9.70e-02 – 1.79e+01	**1766**, 1797	*	*	*	*	*F*HT	*	*	*
	1.61e-01 – 1.72e+01	1927, **1988**	*	*	*	*	*	*	*	*
	1.61e-01 – 1.72e+01	2113	*	*	*	*	*	*	*	*
	1.09e-01 – 1.78e+01	2366	*	*	*	*	*	*	*	*
	2.80e-02 – 1.73e+01	2406					F			H
	3.40e-02 – 1.46e+01	2705, **2710**	*	*	*	*	*	T	*	*
	2.40e-02 – 1.24e+01	3037	T		*		*F*HT			*

Larivière, Vassh, Deng, Wang, and Surman 26 (submitted, arXiv:2605.17213)

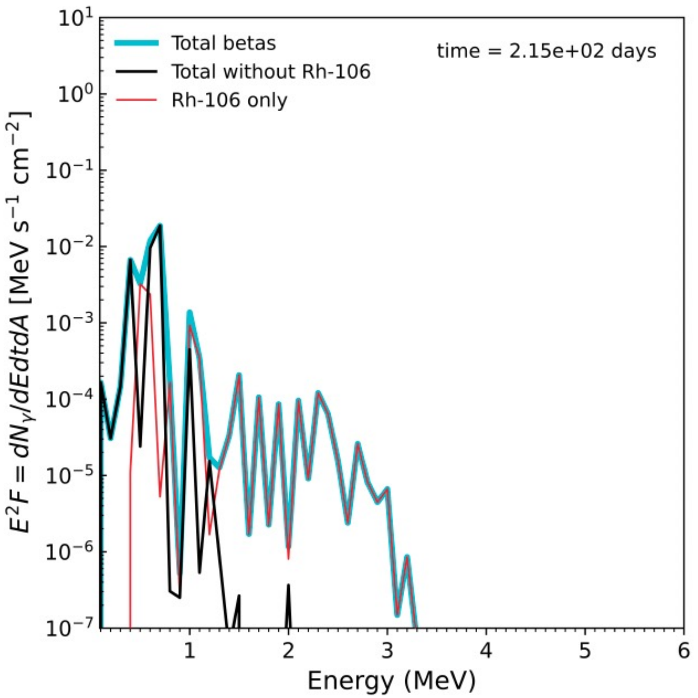

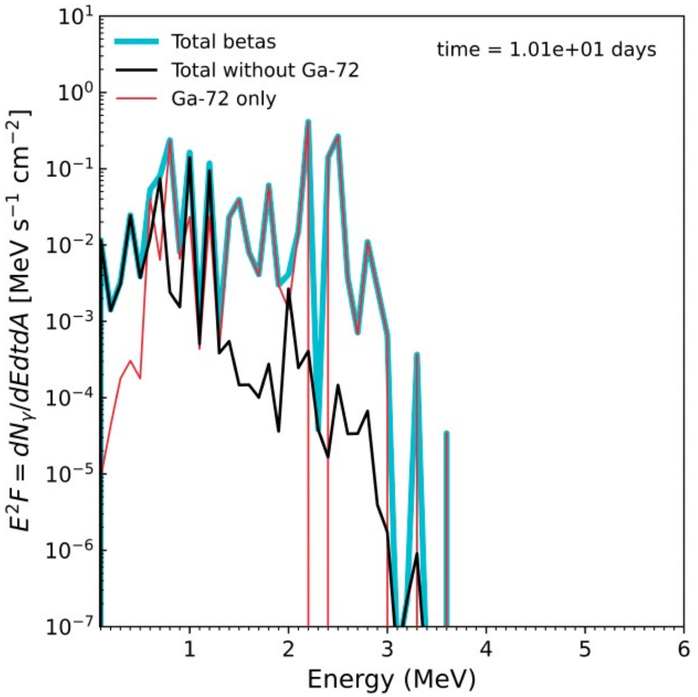

Detailed analysis of competition between fission gammas and β-decay emission

Top: very n-rich case (Ye=0.01),
bottom: moderately n-rich case (Ye=0.19)

Energies >3.5 MeV dominated by prompt fission gammas over beta-decay emission at times > 1 day in all calculation variations; almost all higher energy beta-decay lines from fission daughters (flux below prompt); notable exception Rb-88's 4.7 MeV strong line (only at earlier times)

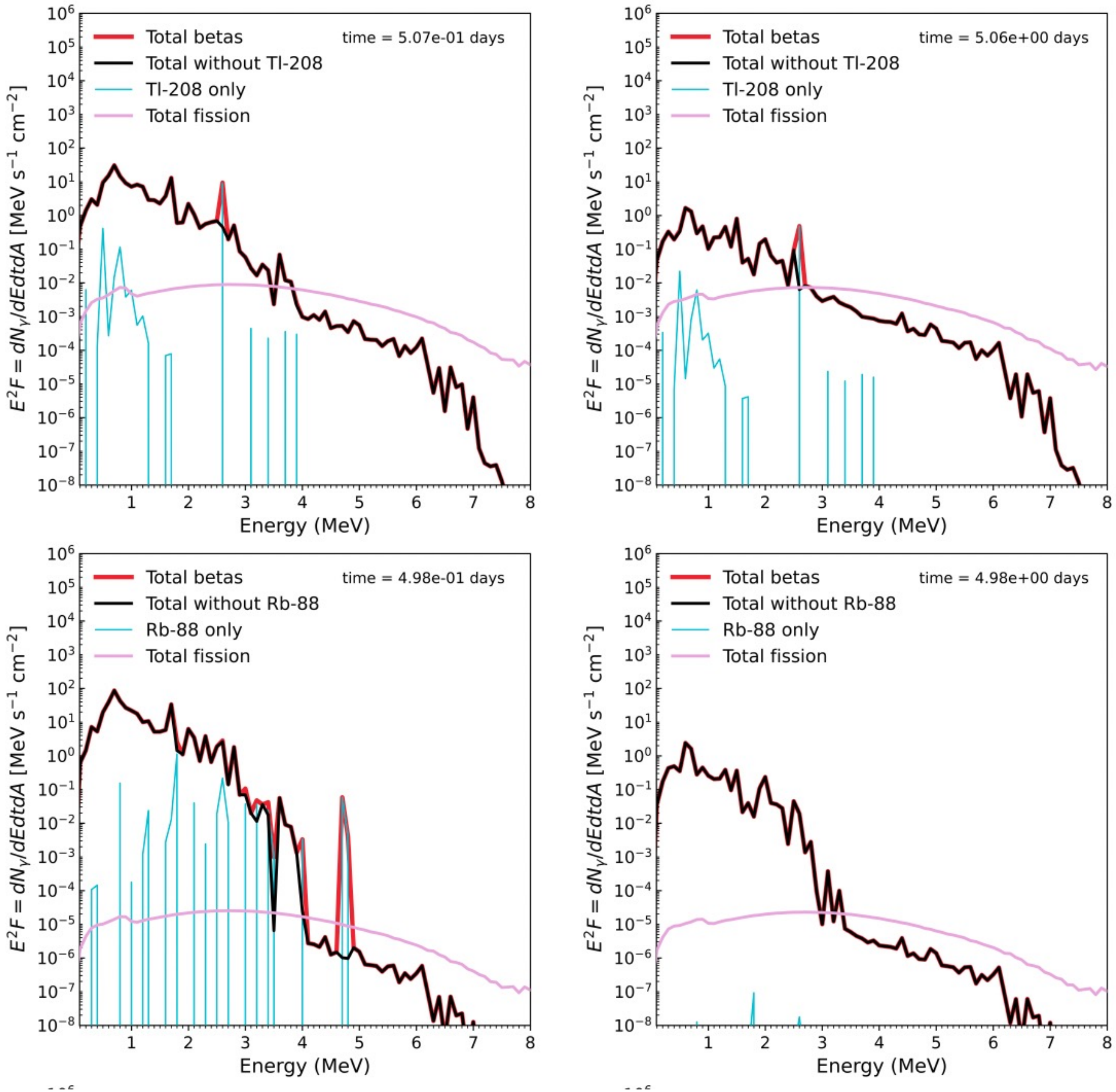

Larivière, Vassh, Deng, Wang, and Surman 26 (submitted, arXiv:2605.17213)

Towards refining calculations of *r*-process observables

Solar system abundances
as observed in meteorites

Metal-poor star abundances

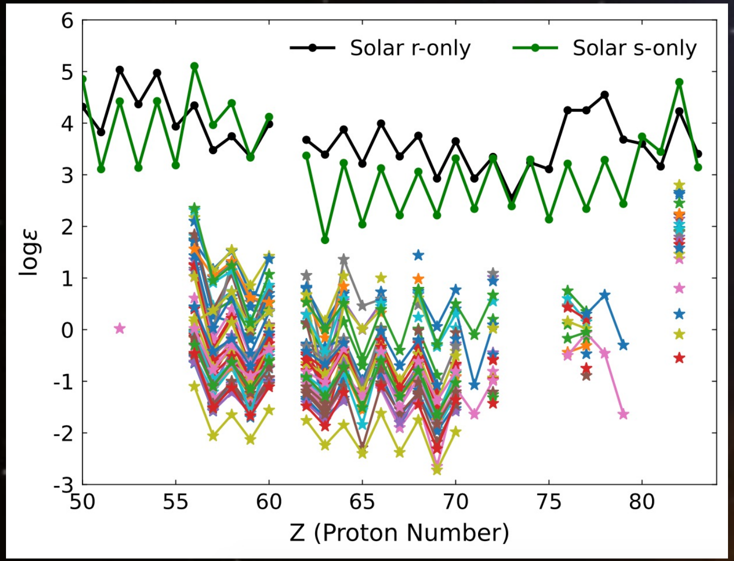

EM emission from
rare events

Telescope
Campaigns

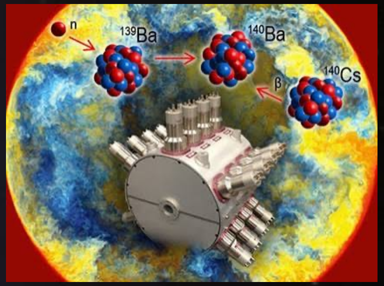

Nuclear
Experiment

Machine
Learning

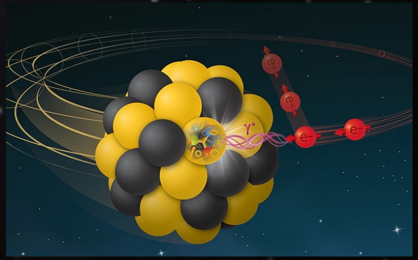

Nuclear
Theory

TITAN mass measurements: Cs, Ba

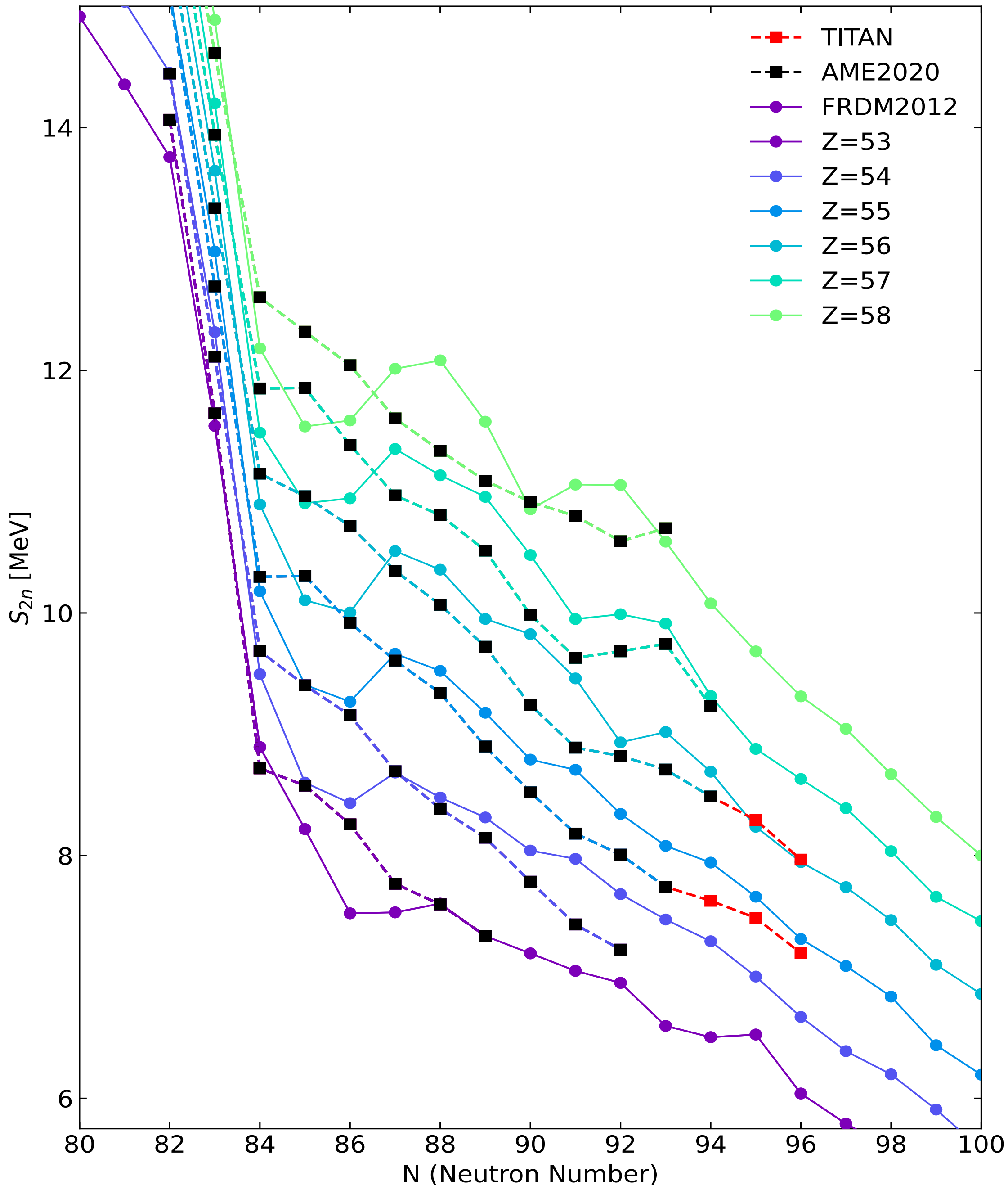

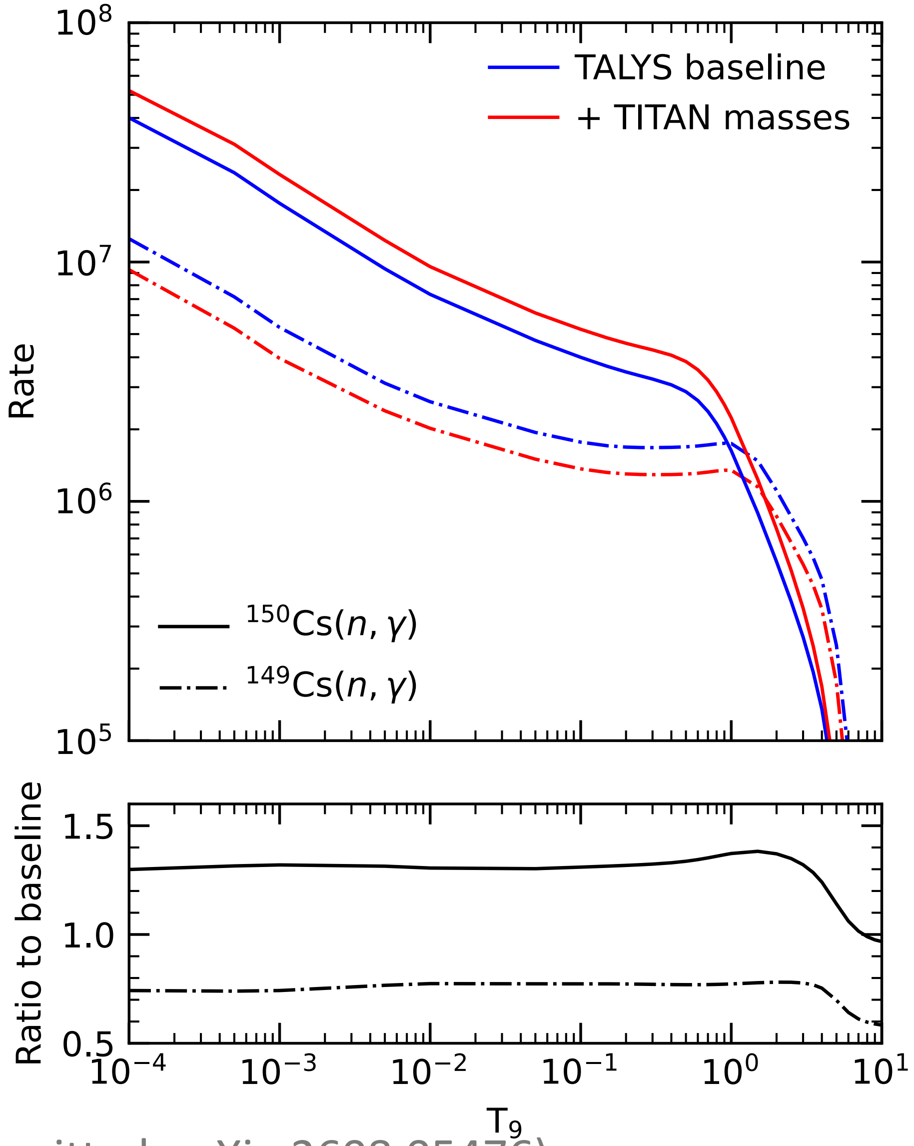

Yeh, Cordova, Wang, et al (including Vassh) (submitted, arXiv:2608.05476)

TITAN mass measurements: Cs, Ba

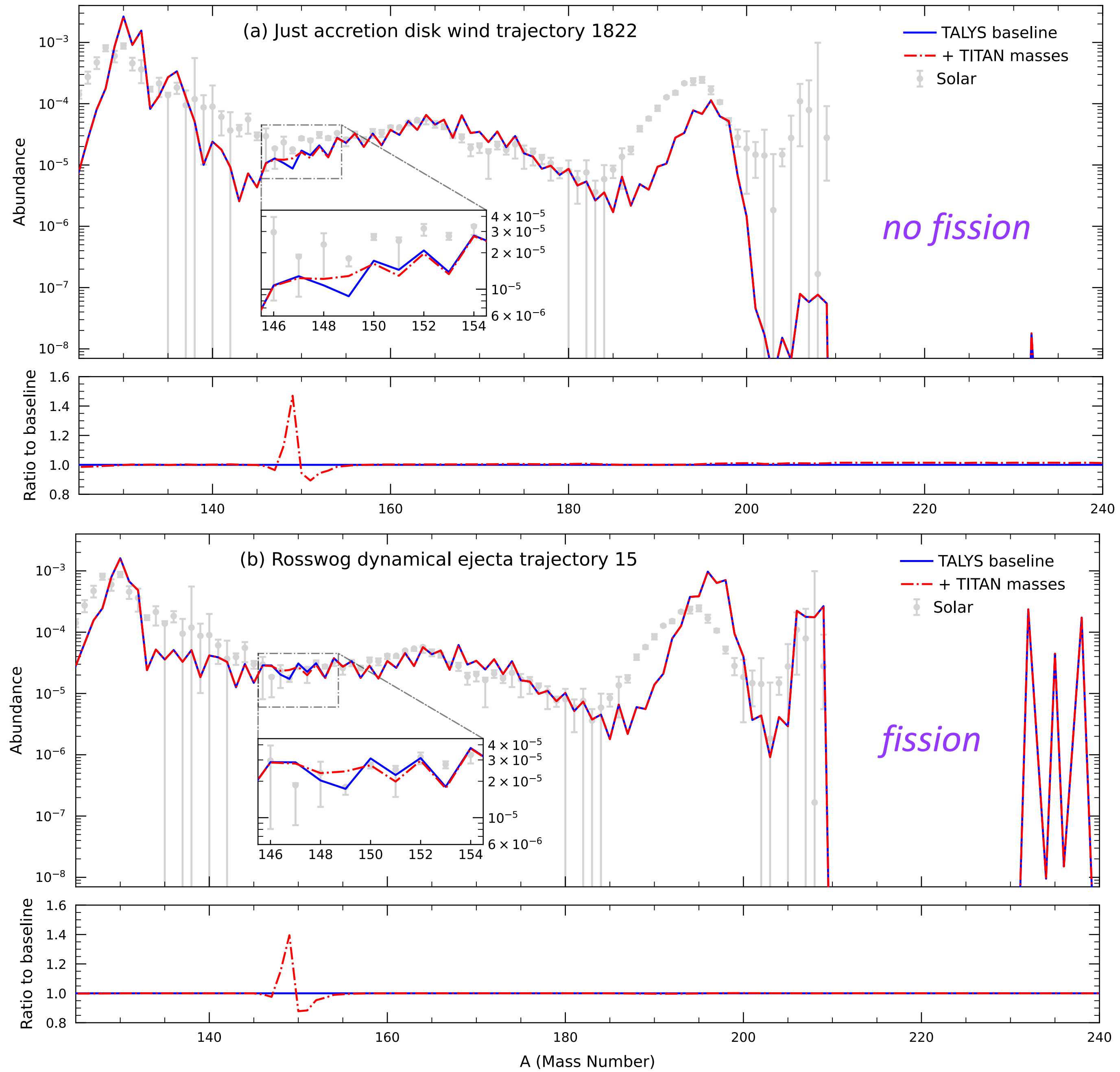

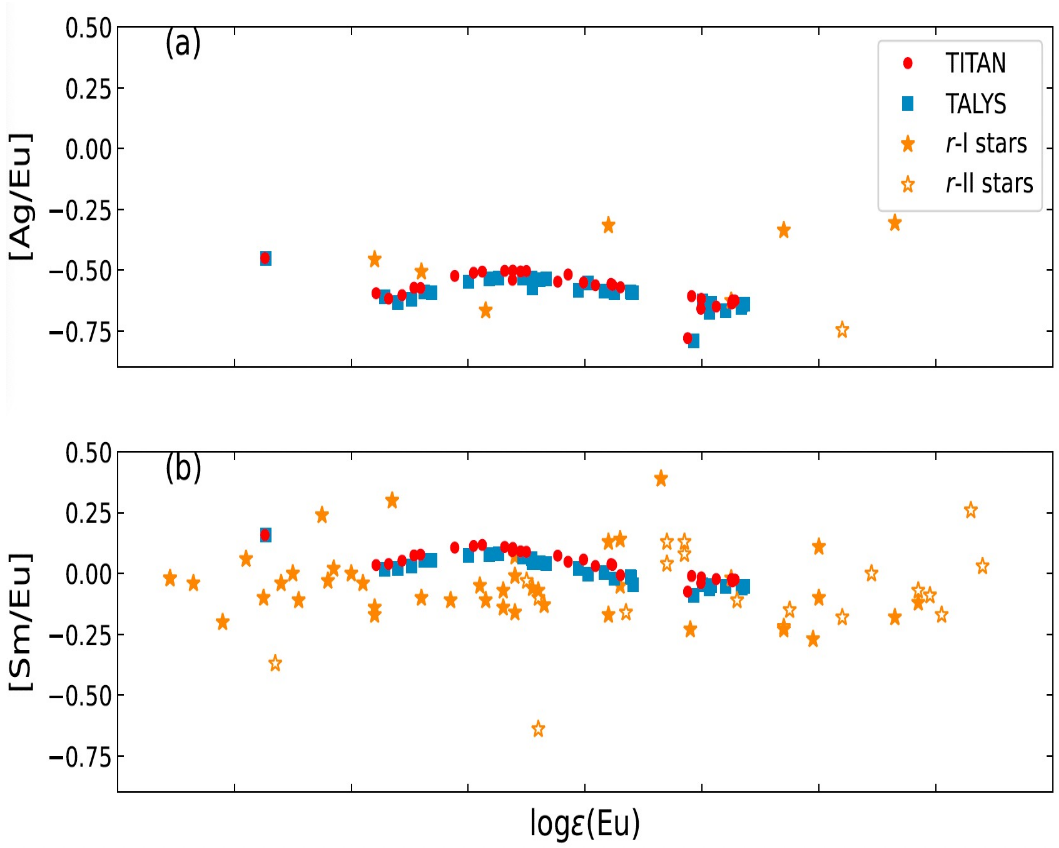

Affects comparisons to Solar and metal-poor star trends for key r-dominated lanthanide abundances in cases both w/ and w/o fission deposition

Yeh, Cordova, Wang, et al (including Vassh) (submitted, arXiv:2608.05476)

Towards refining calculations of *r*-process observables

Solar system abundances as observed in meteorites

Metal-poor star abundances

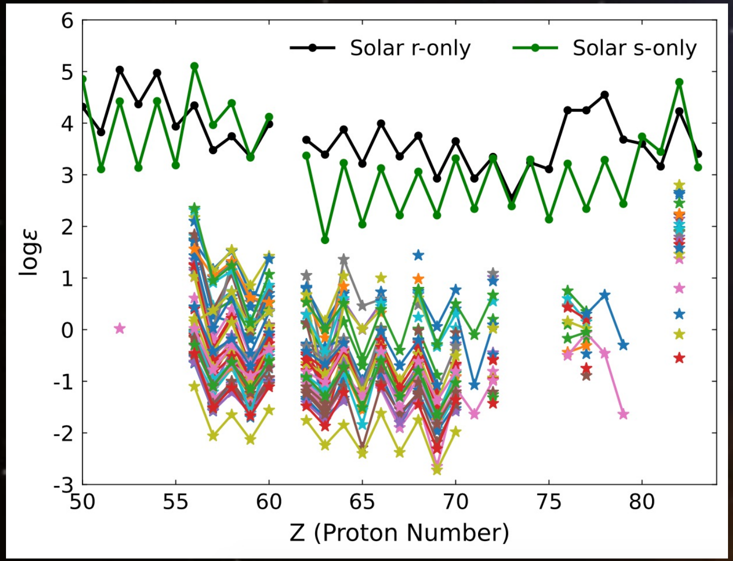

EM emission from rare events

Telescope Campaigns

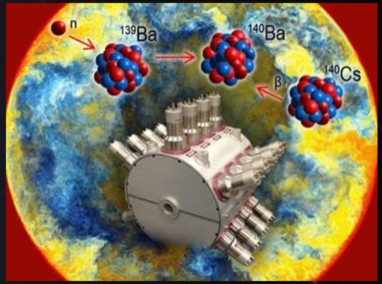

Nuclear Experiment

Machine Learning

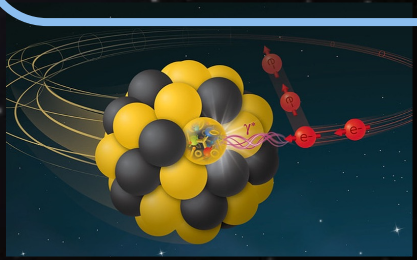

Nuclear Theory

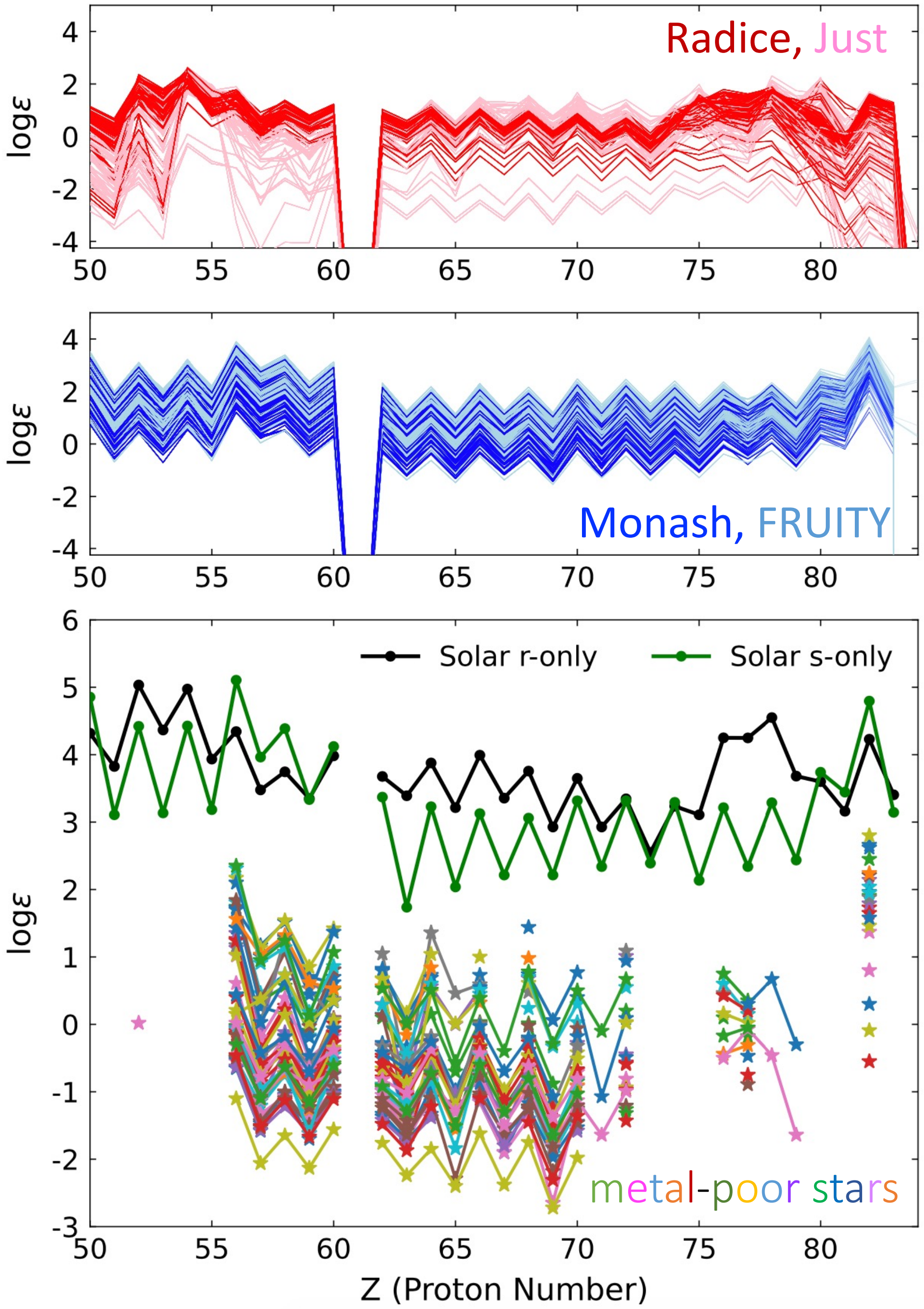

Hydrodynamic simulations of r process and s process events show distinct elemental abundance patterns

Stellar abundance patterns are available for > 100 metal-poor stars

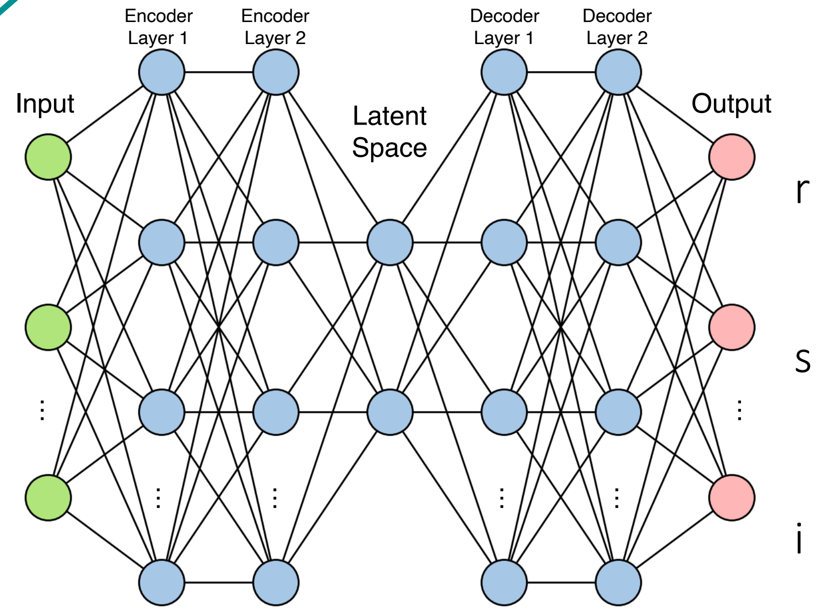

Machine learning can classify patterns = *Machine learning can classify stars*

Ba, La, Ce, Pr, Nd, Sm, Eu, Dy, Er (Z=56, 57, 58, 59, 60, 62, 63, 66, 68) as one feature set. Also considered a second feature set with Er replaced by Pb.

Vassh, Wang, Woloshyn, Kutchera, Larivière, Majic, Côté (ApJ 2025, arXiv:2505.14563)

Machine learning to classify metal-poor stars as r or s

Binary classifier
(supervised training on r *and* s)

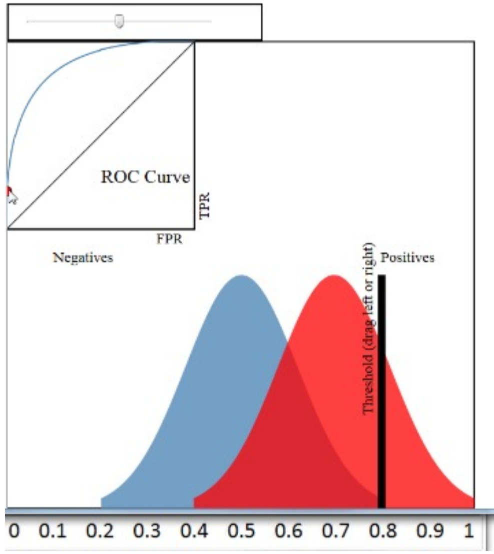

True Positive Rate = 50 / 250 = 0.2

False Positive Rate = 0 / 250 = 0

Plot on ROC Curve: (x, y) = (0, 0.2)

UBC/TRIUMF PhD student Yilin Wang

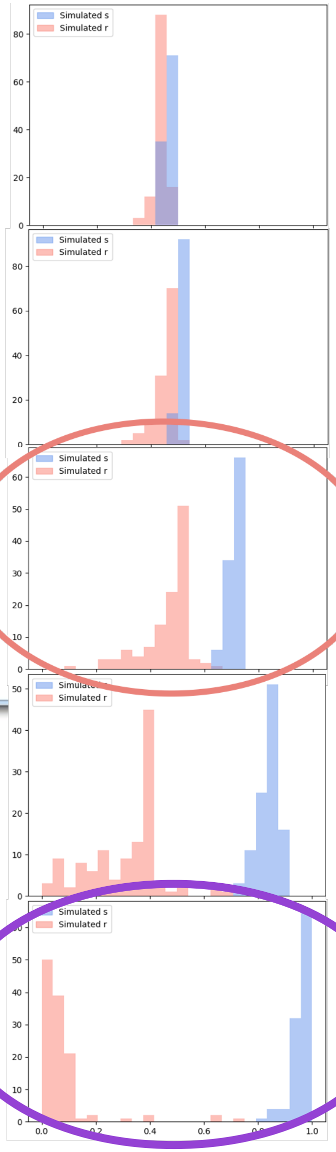

More epochs

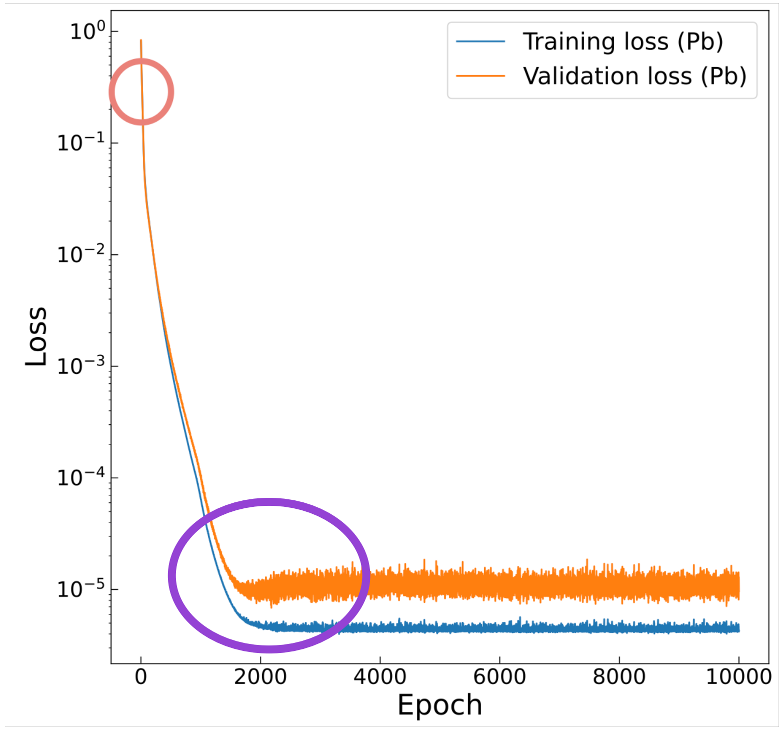

Binary Cross Entropy Loss Function

$$\mathrm{BCE} = -\frac{1}{N}\sum_{i=1}^{N}\left[y_i \log(p_i) + (1-y_i)\log(1-p_i)\right]$$

- N is the number of observations
- y_i is the actual binary label (0 or 1) of the i^{th} observation.
- p_i is the predicted probability of the i^{th} observation being in class 1

Vassh, Wang, Woloshyn, Kutchera, Larivière, Majic, Côté (ApJ 2025, arXiv:2505.14563)

Machine learning to classify metal-poor stars as r or s

One-class classifier
(unsupervised training on r *or* s)

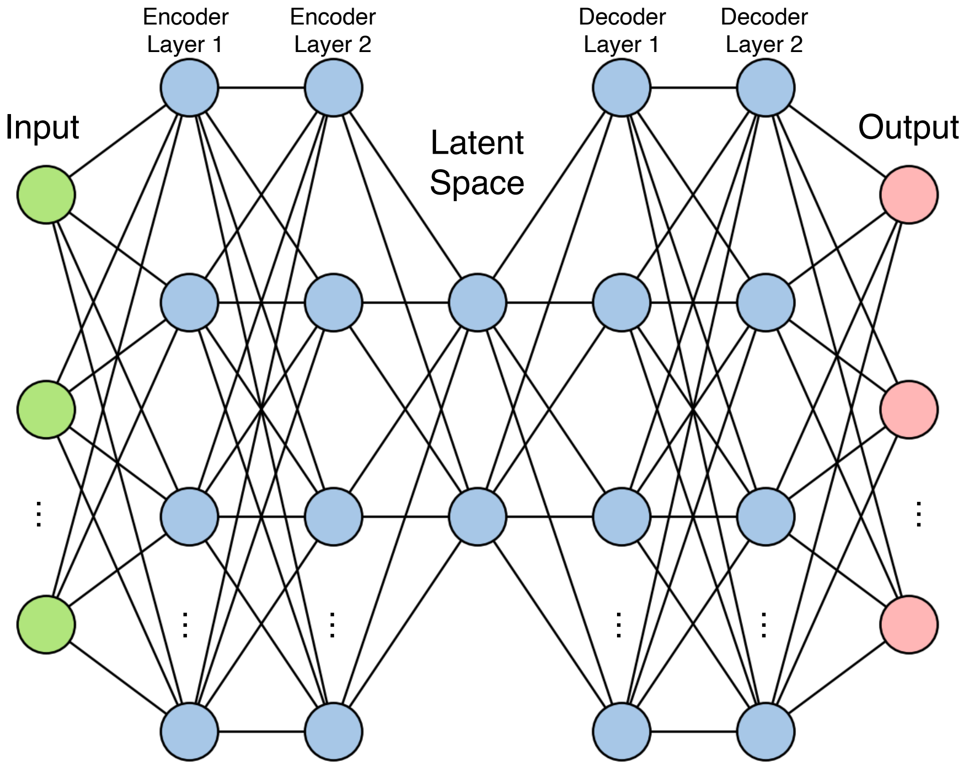

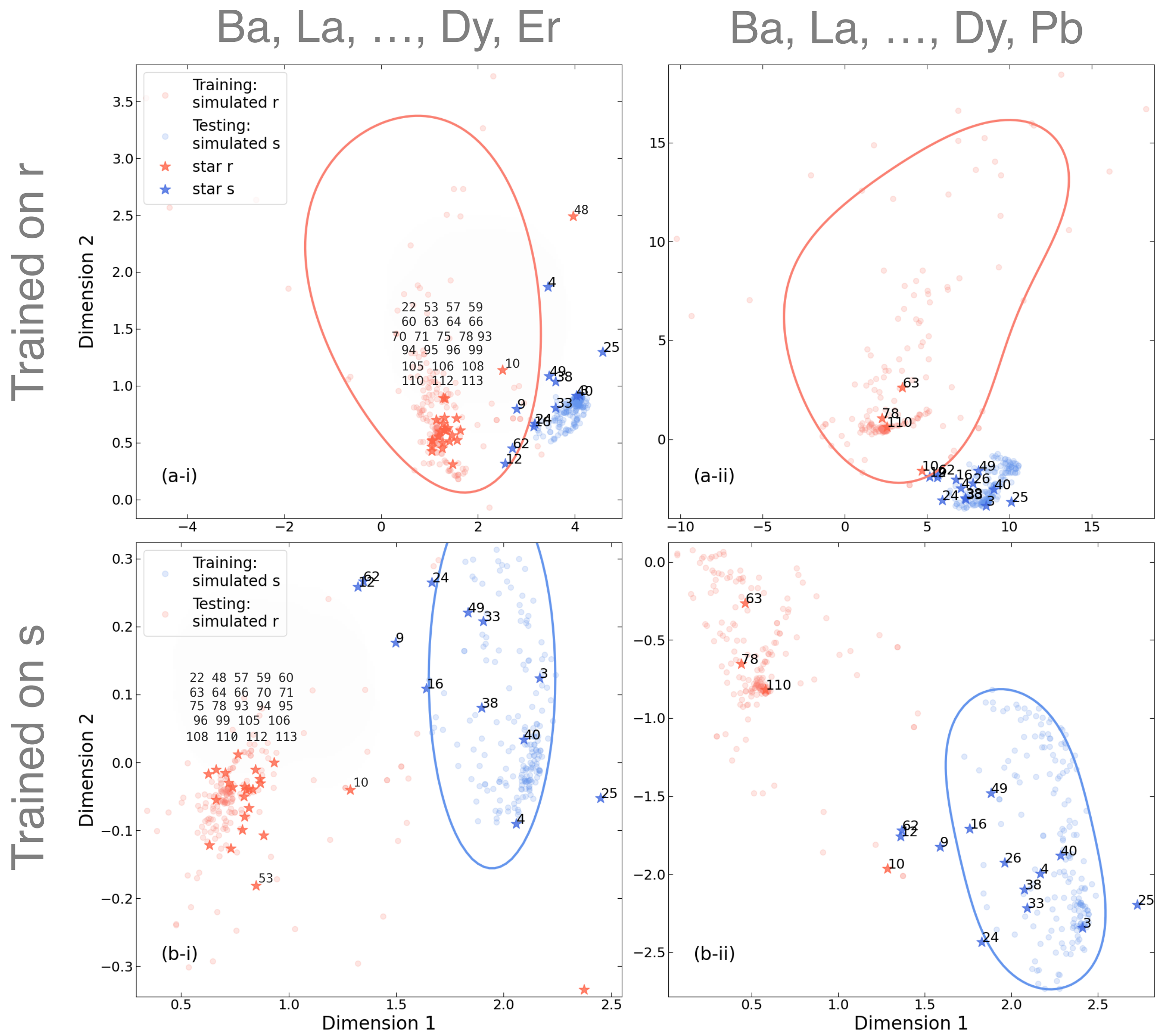

Vassh, Wang, Woloshyn, Kutchera, Larivière, Majic, Côté (ApJ 2025, arXiv:2505.14563)

Machine learning to classify metal-poor stars as r or s *or i*

* 2/5 i stars fall into the r or s group

* 3/5 i stars are almost *never* identified as r or s!

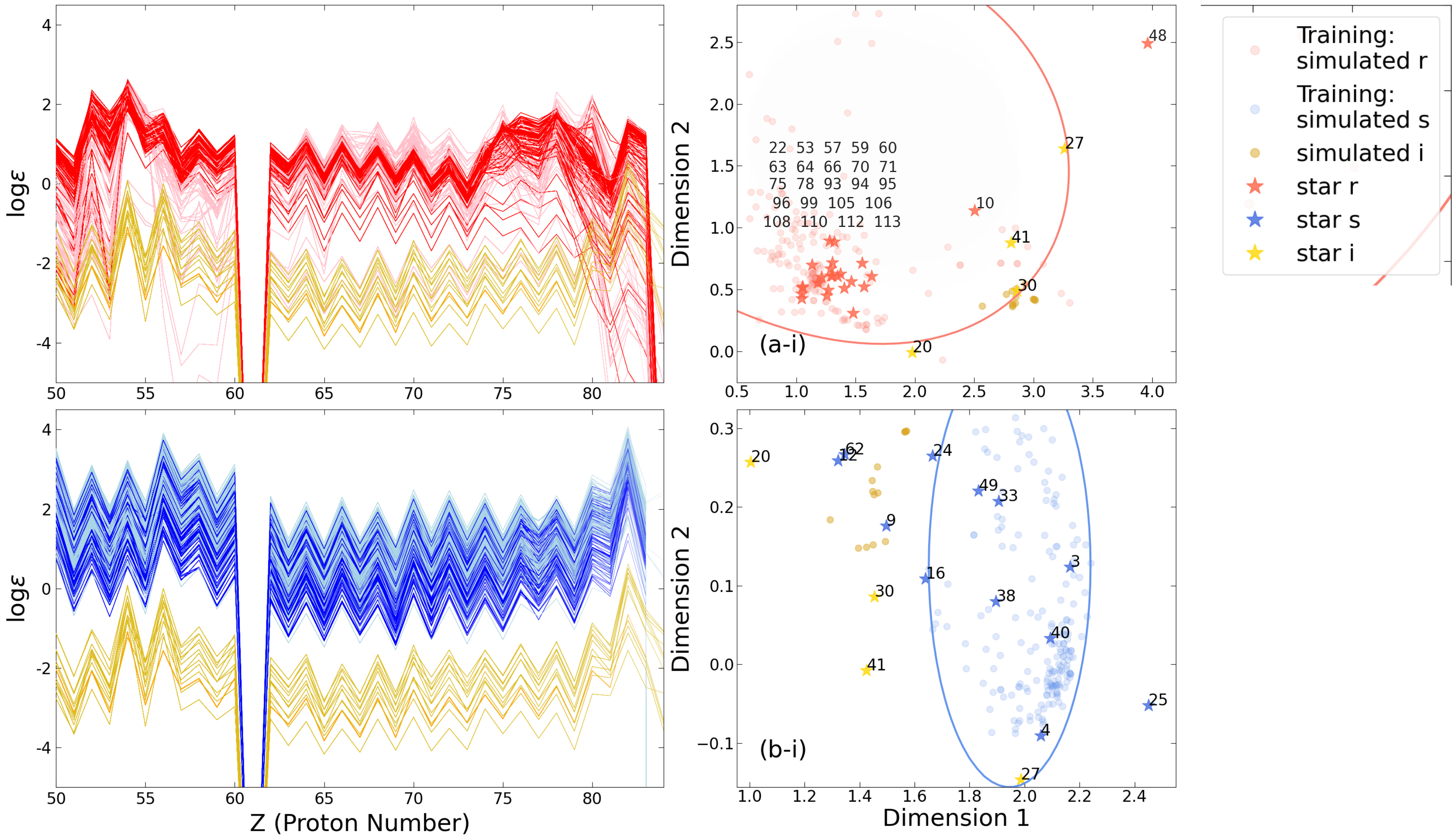

* This application demonstrated that *some stars recently labeled to be of i-process origins are actually compatible with r or s groups* BUT *some stars were not found to belong to either group* → **first ML predictions of a process beyond r and s**

Vassh, Wang, Woloshyn, Kutchera, Larivière, Majic, Côté (ApJ 2025, arXiv:2505.14563)

ML feature importance: which elemental abundances are most informative?

First consider the feature set without Pb: Ba, La, Ce, Pr, Nd, Sm, Eu, Dy, Er

SHAP

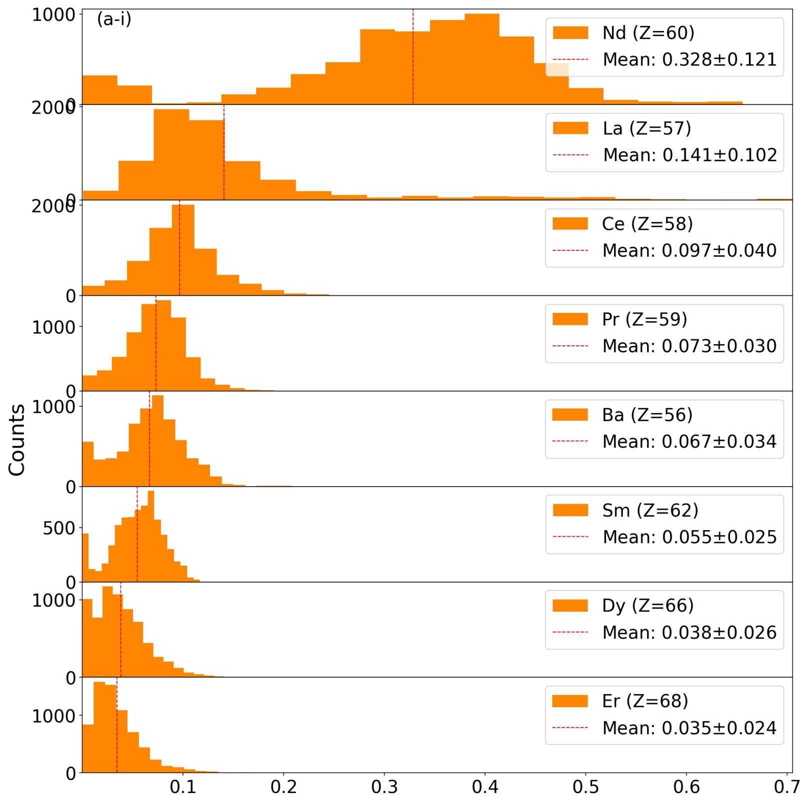

Permutation Feature Importance (PFI)

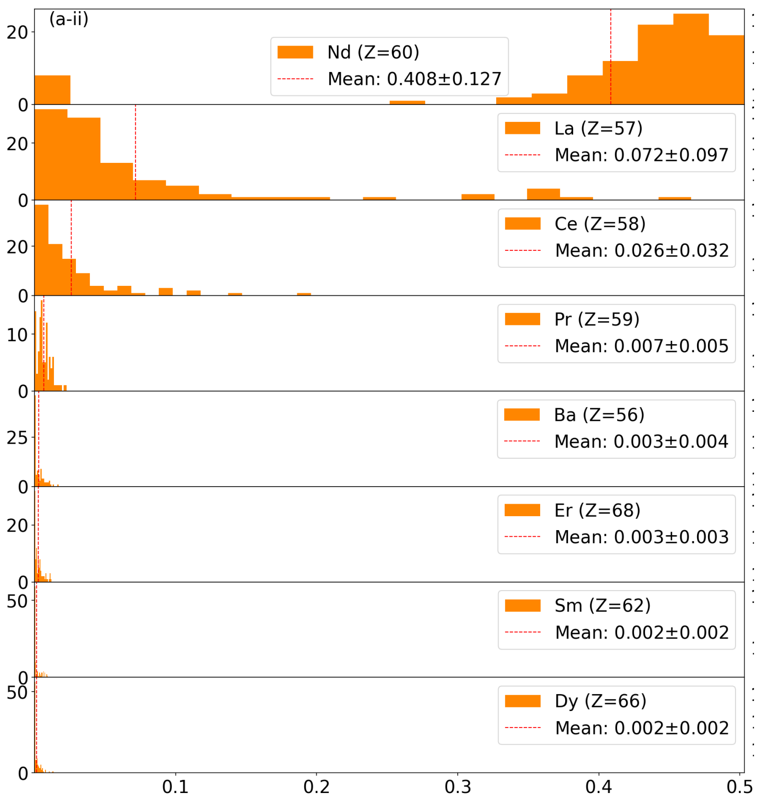

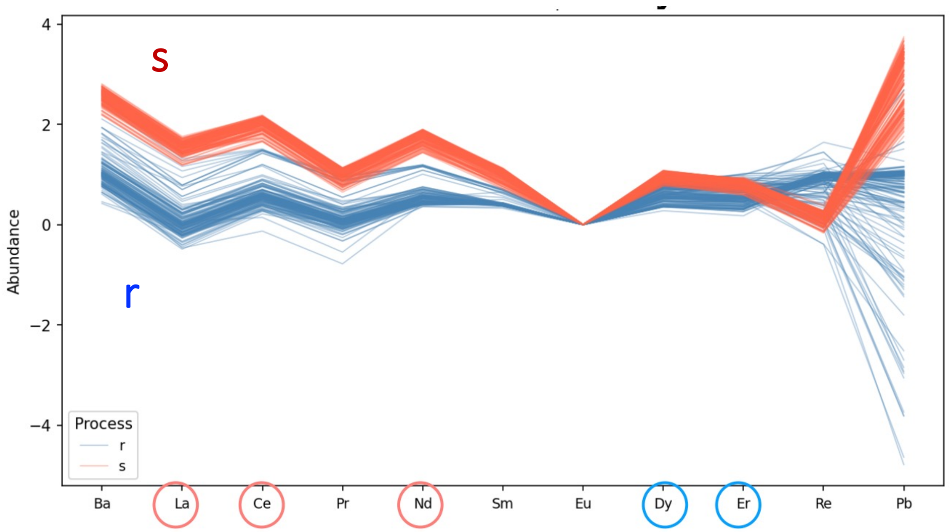

Note SHAP and PFI consider a baseline and then permute values of subsets of features within the data to see how predictions change relative to this baseline; must take care to not be skewed by unphysical combinations!

Wang, Vassh, Woloshyn+ (in prep)

ML feature importance: which elemental abundances are most informative?

Next consider the feature set with Pb: Ba, La, Ce, Pr, Nd, Sm, Eu, Dy, Pb

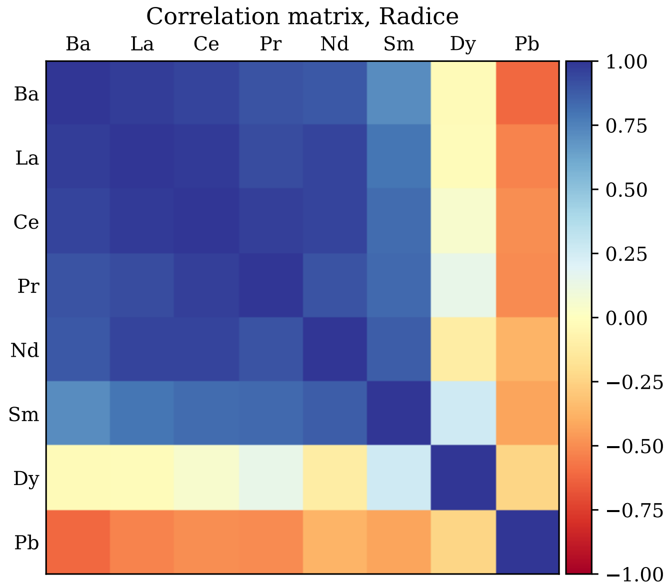

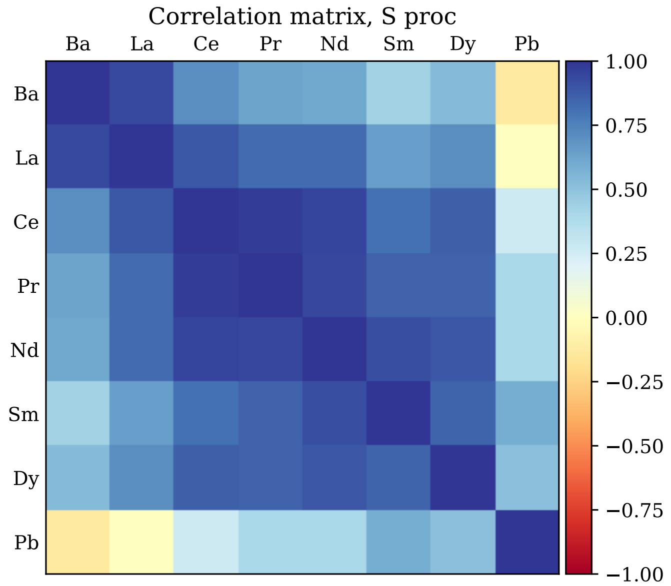

SHAP

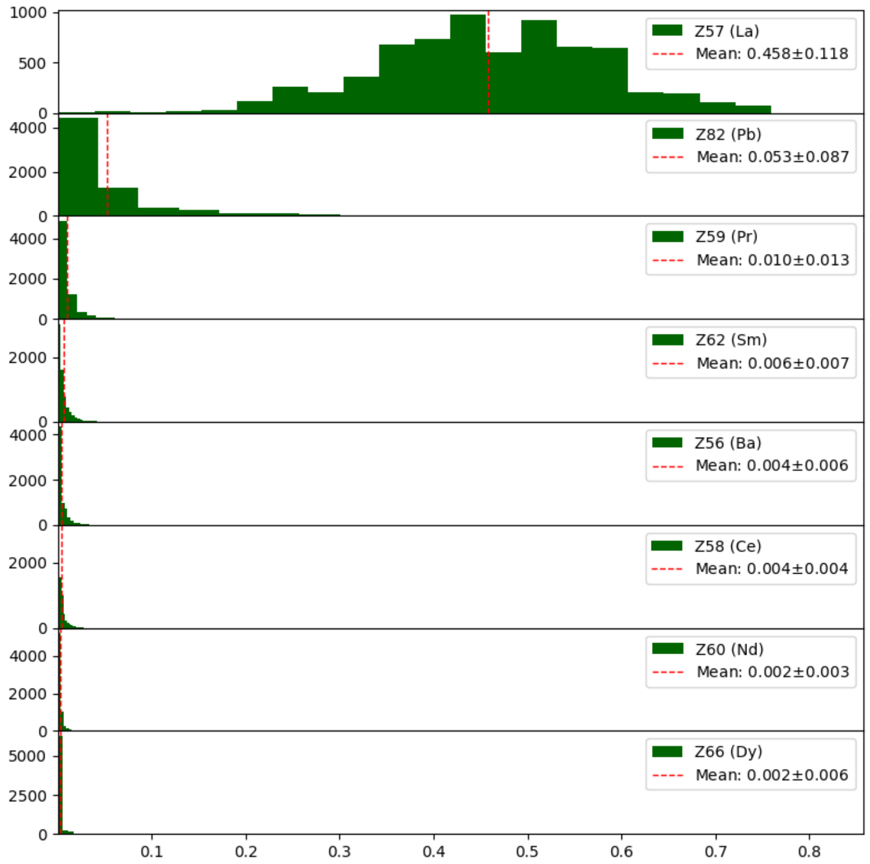

Conditional SHAP (considers covariance when sampling feature values)

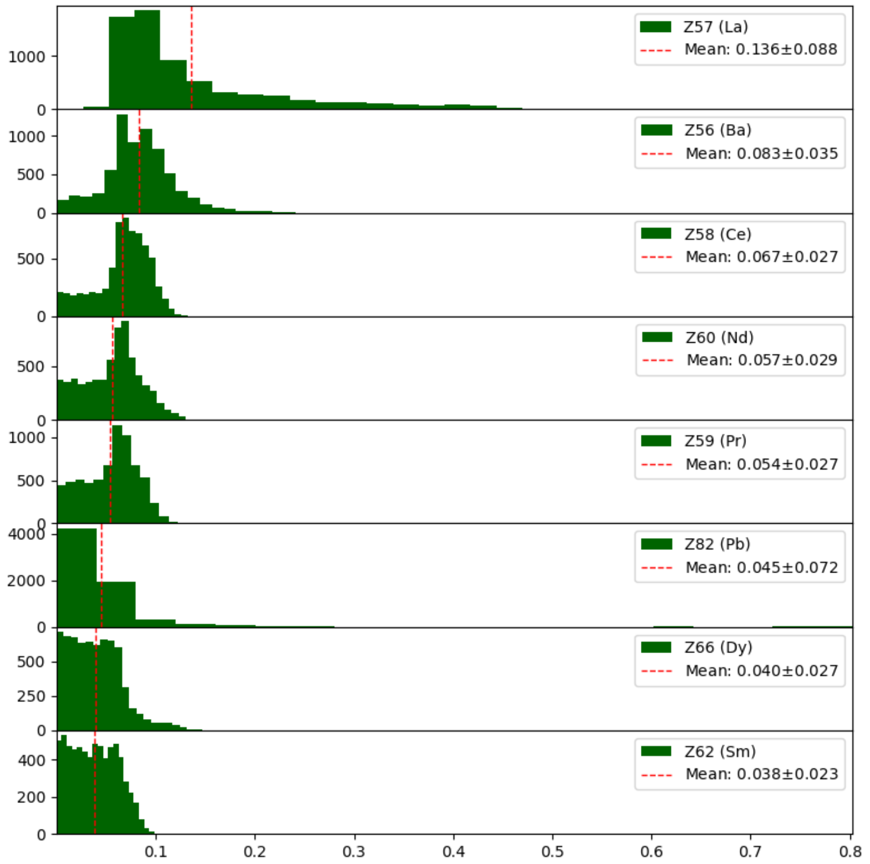

Wang, Vassh, Woloshyn+ (in prep)

Using ML to predict masses across the nuclear chart

Mixed Density Neural Network to predict nuclear masses

Features	Description
N	Neutron number
Z	Proton number
A	Mass number
P_{asym}	Asymmetry correction
V_n	Valence neutron
V_p	Valence proton

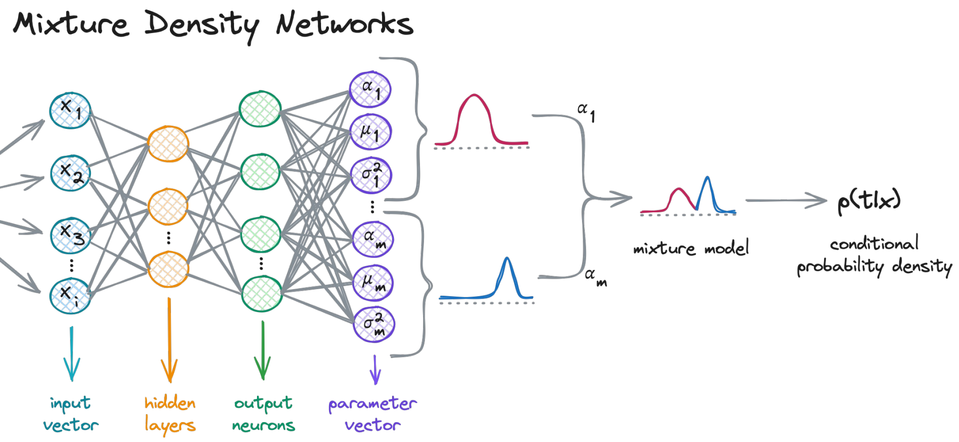

N3AS postdoc
Mengke Li

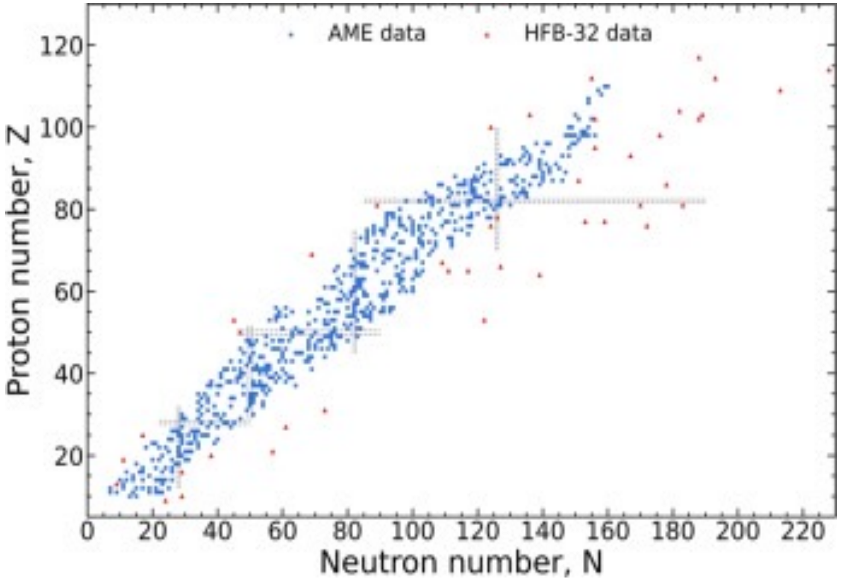

Pb isotopic chain

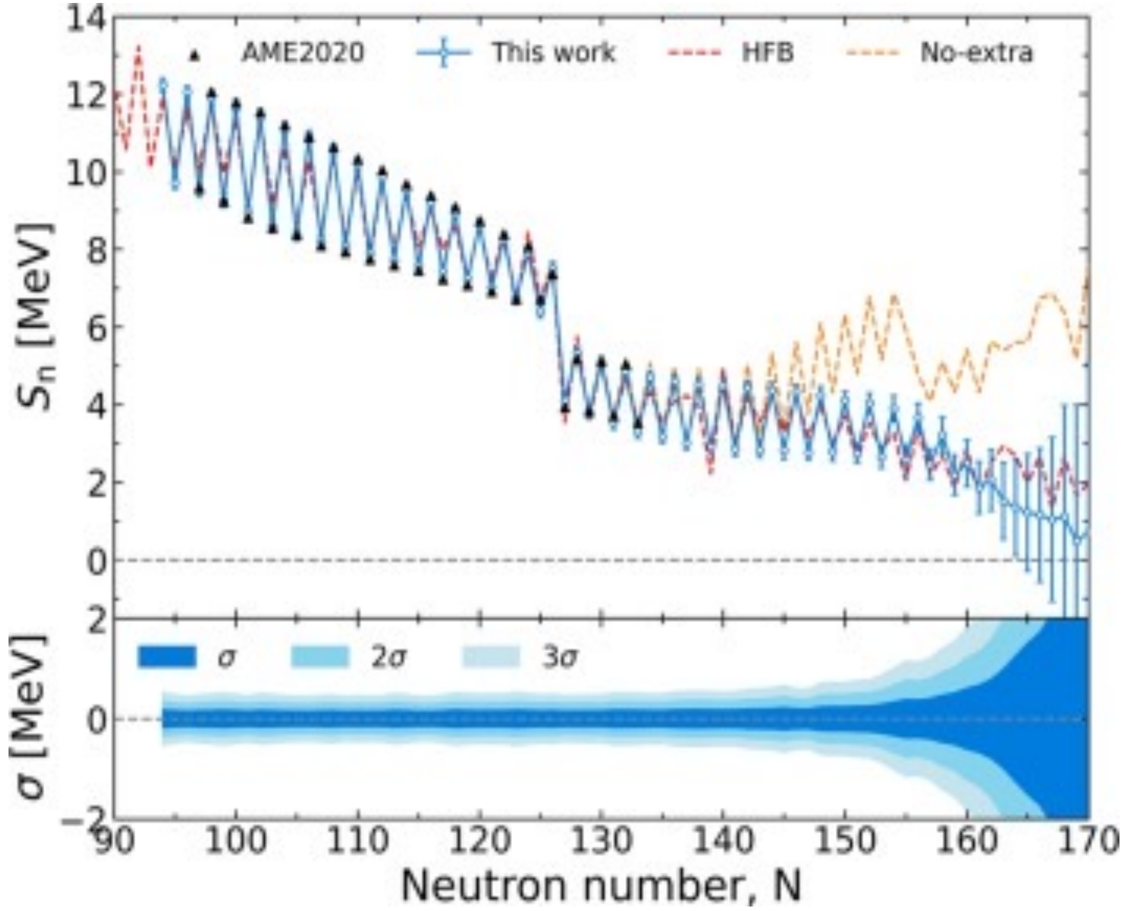

Li, Sprouse, Meyer, and Mumpower
(Phys. Lett. B 2024)

Using ML with Solar and metal-poor star abundances to constrain masses

Find the subset of predicted global models which are physical and would match observation if a given astrophysical event were both the source of main *r*-process elements for our Sun and metal-poor star HD22295

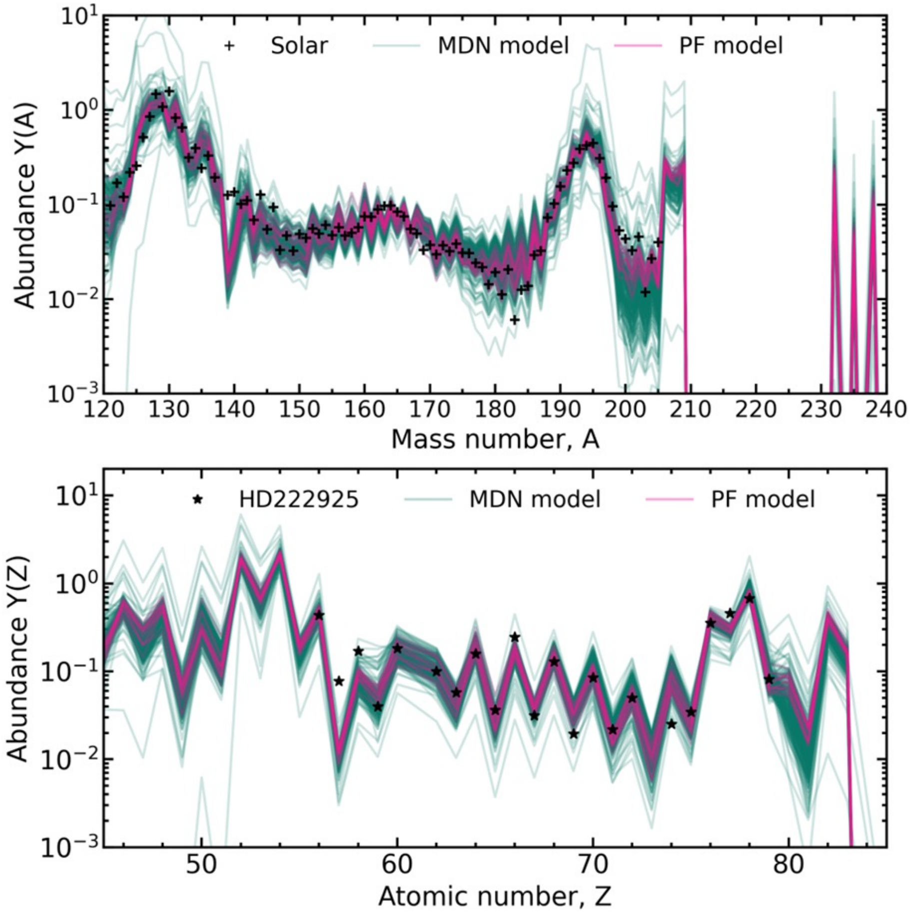

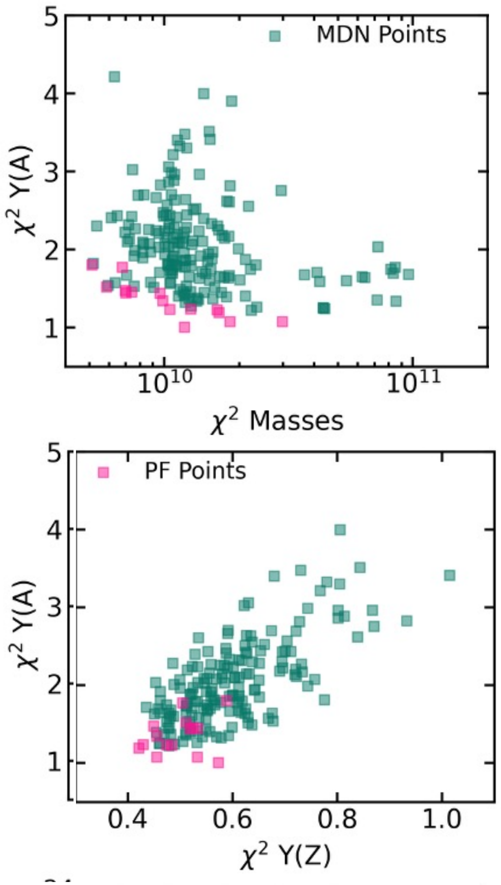

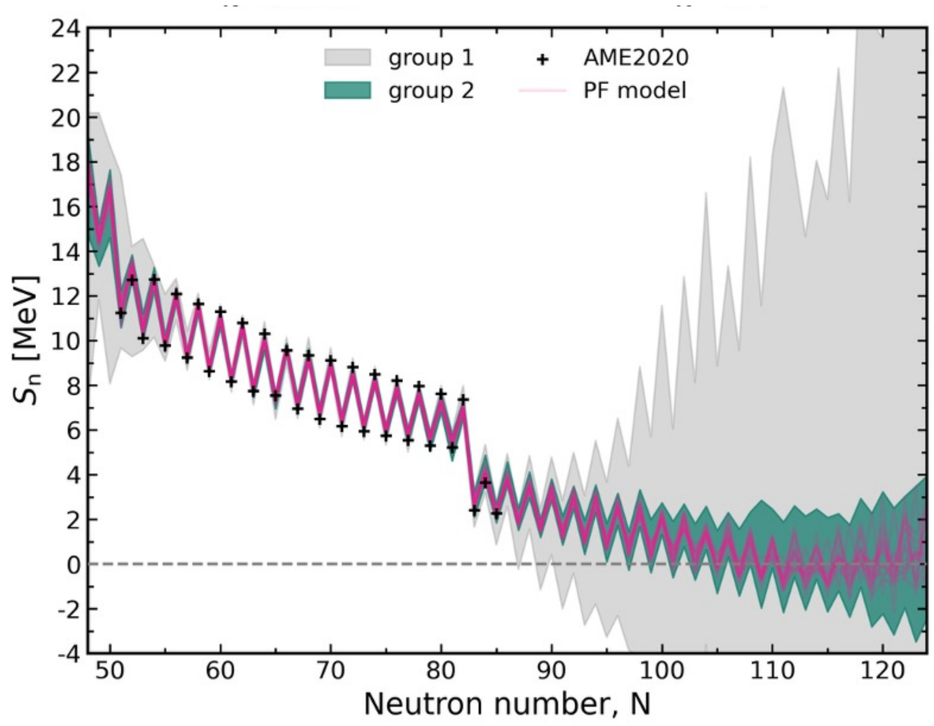

Li, Mumpower, Vassh and Surman (Phys. Rev. Res. Lett. 2025)

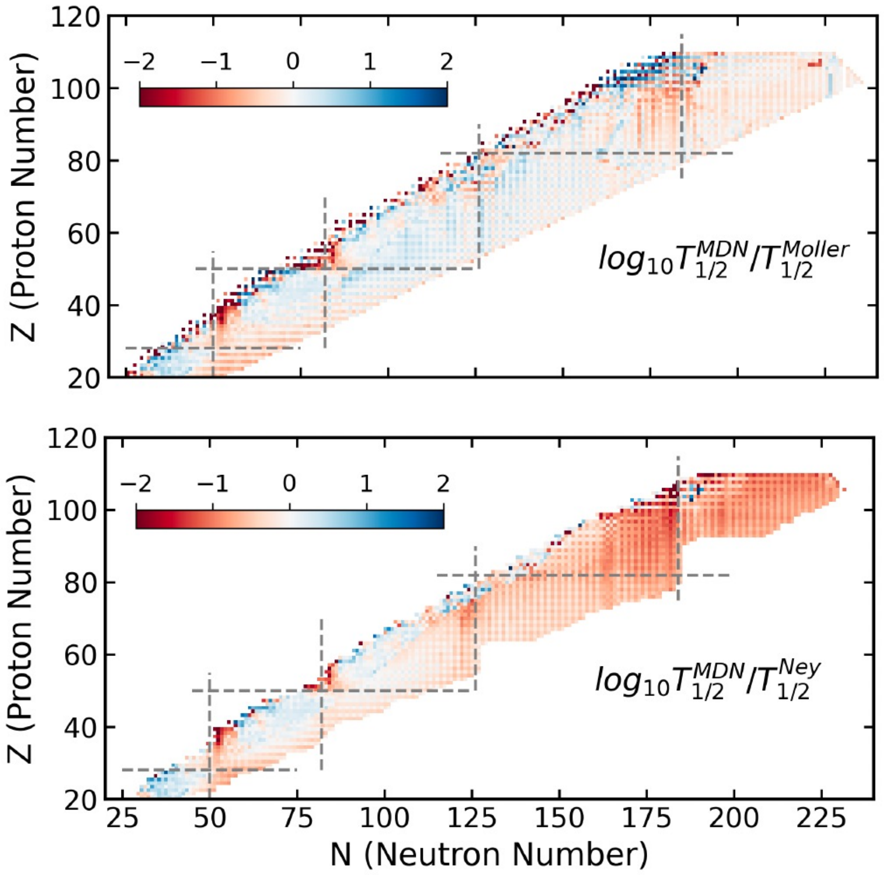

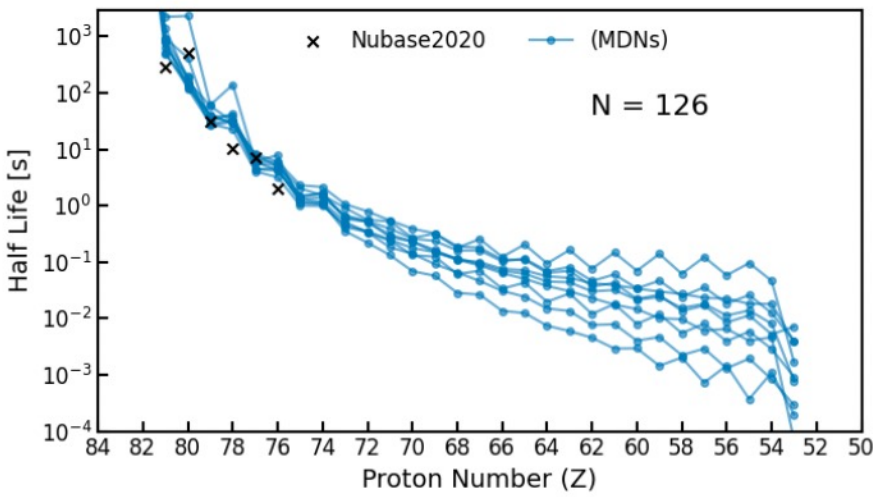

Using ML to infer β-decay half-lives and uncertainties

Li, Wang, Engel, Mumpower, Vassh and Surman (in prep.)

Using ML to infer β-decay half-lives and uncertainties

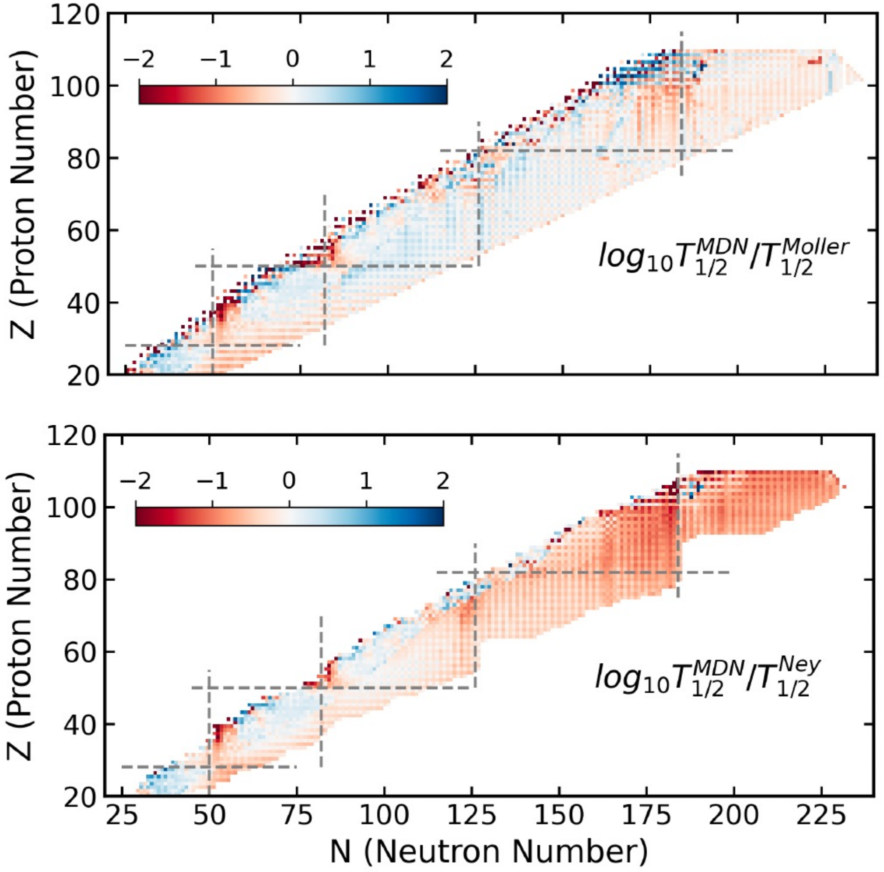

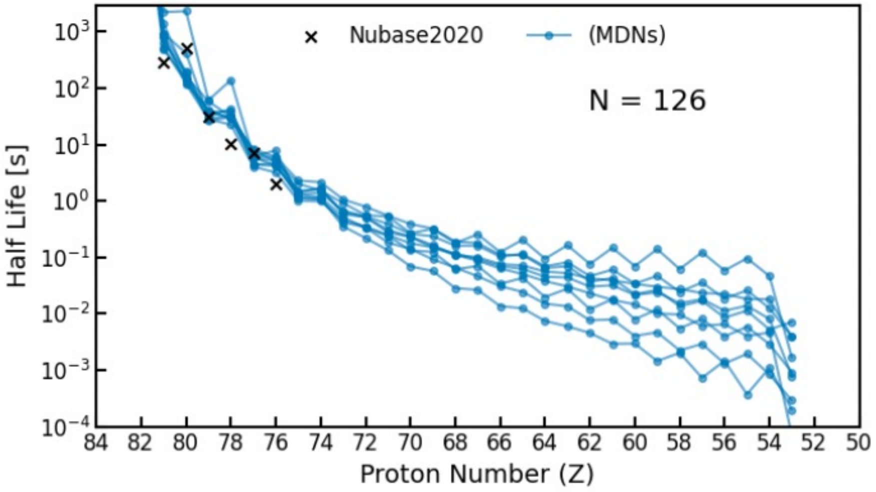

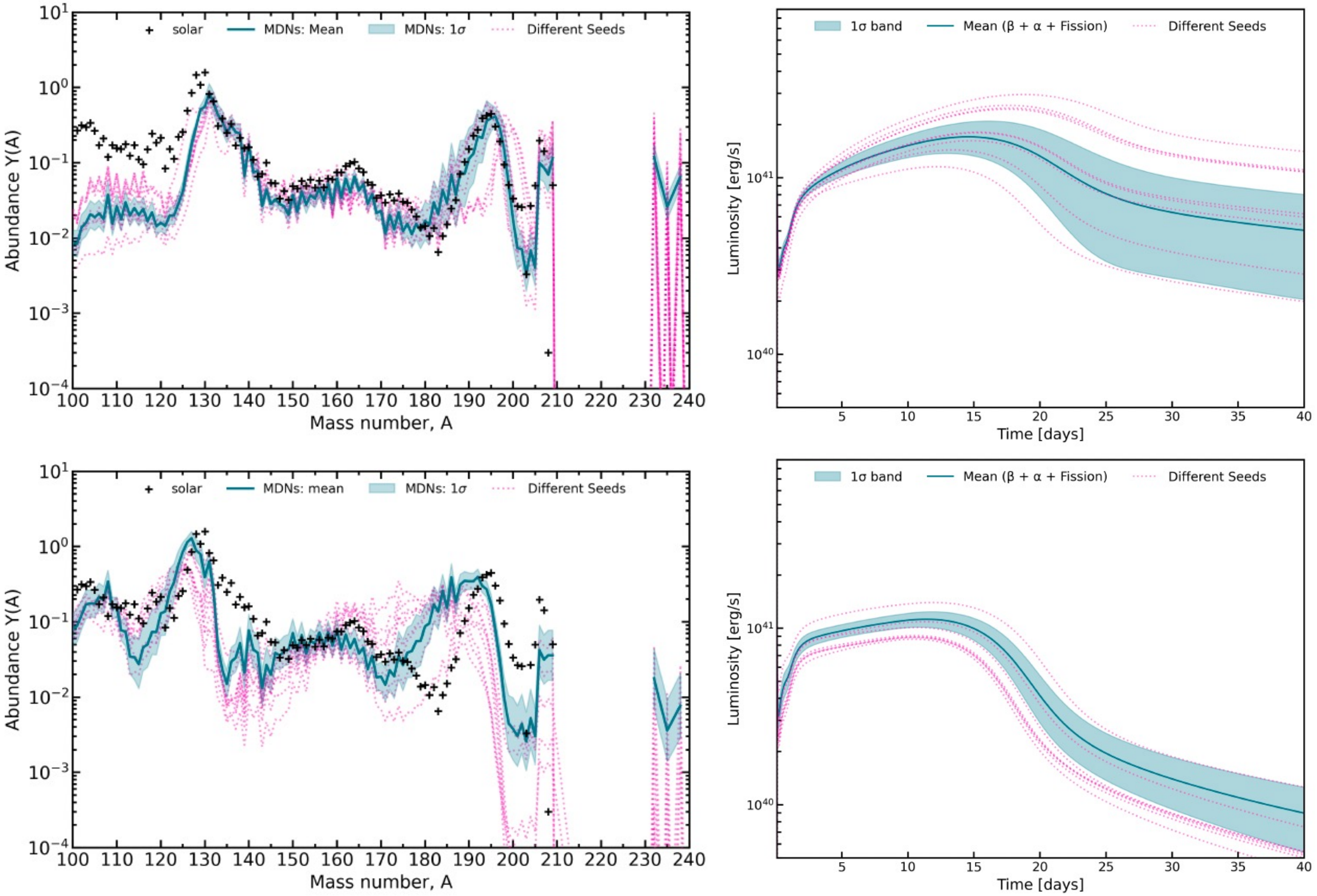

Li, Wang, Engel, Mumpower, Vassh and Surman (in prep.)

Towards refining calculations of *r*-process observables

Solar system abundances as observed in meteorites

Metal-poor star abundances

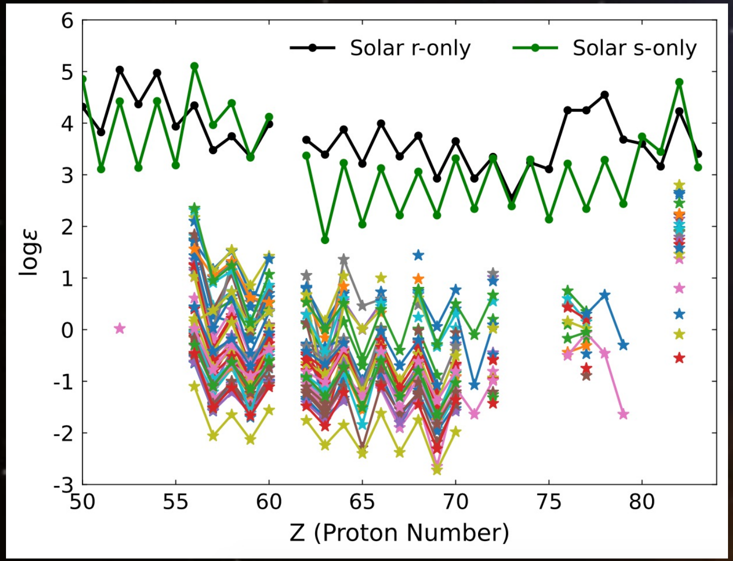

EM emission from rare events

Telescope Campaigns

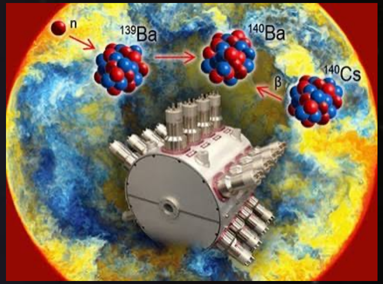

Nuclear Experiment

Machine Learning

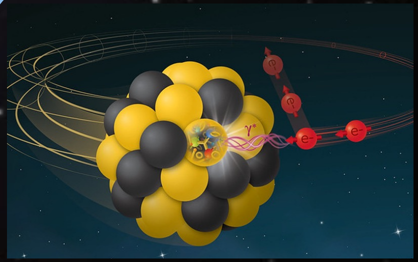

Nuclear Theory

Ab initio nuclear theory: new reach into *r*-process nuclei

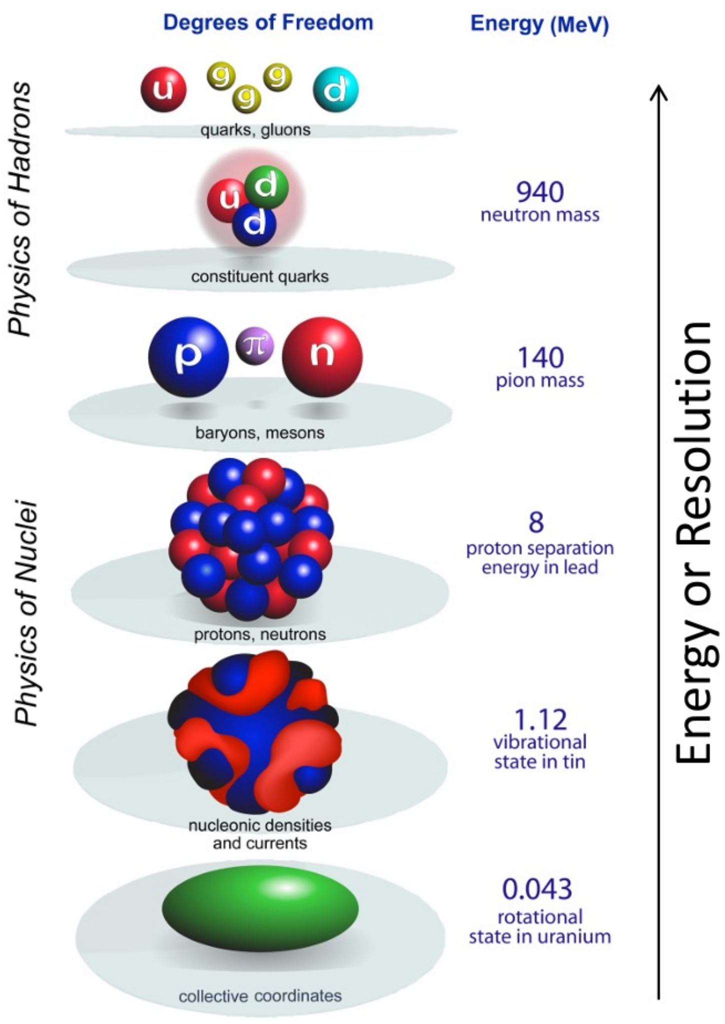

Fig.: Bertsch, Dean, Nazarewicz (2007)

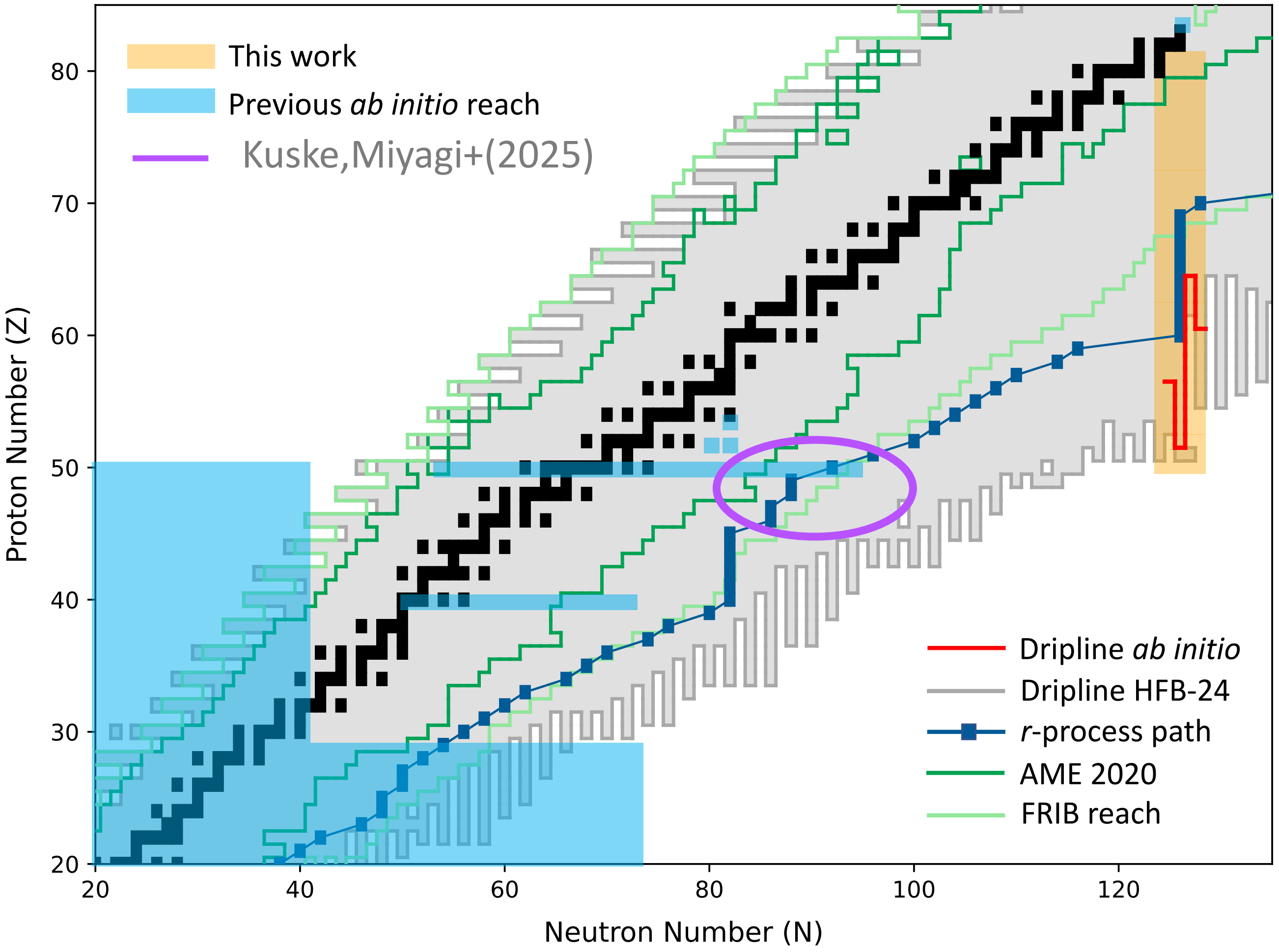

Hu, Larivière, Vassh, and Holt (in prep)

Ab initio nuclear theory: new reach into *r*-process nuclei

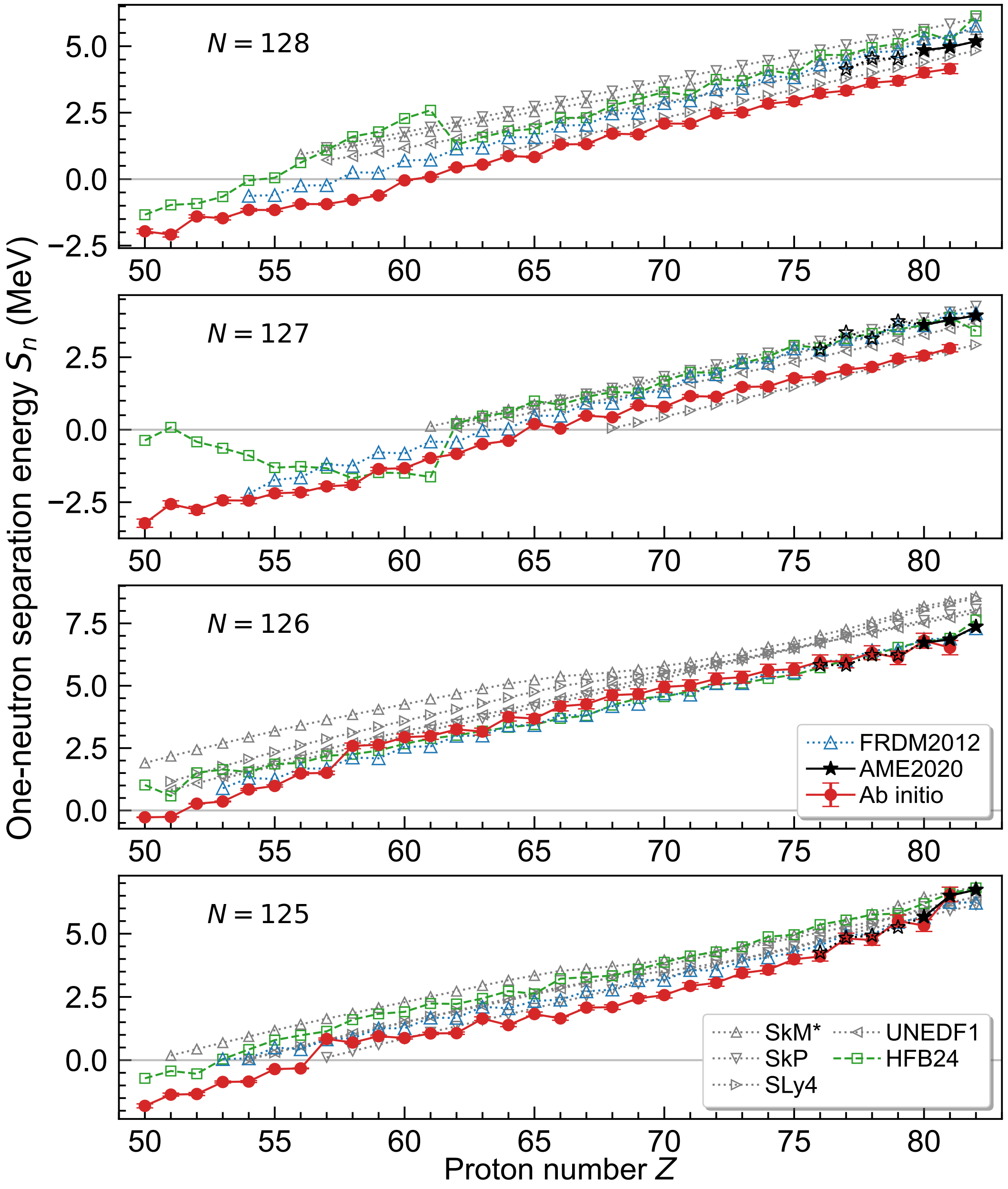

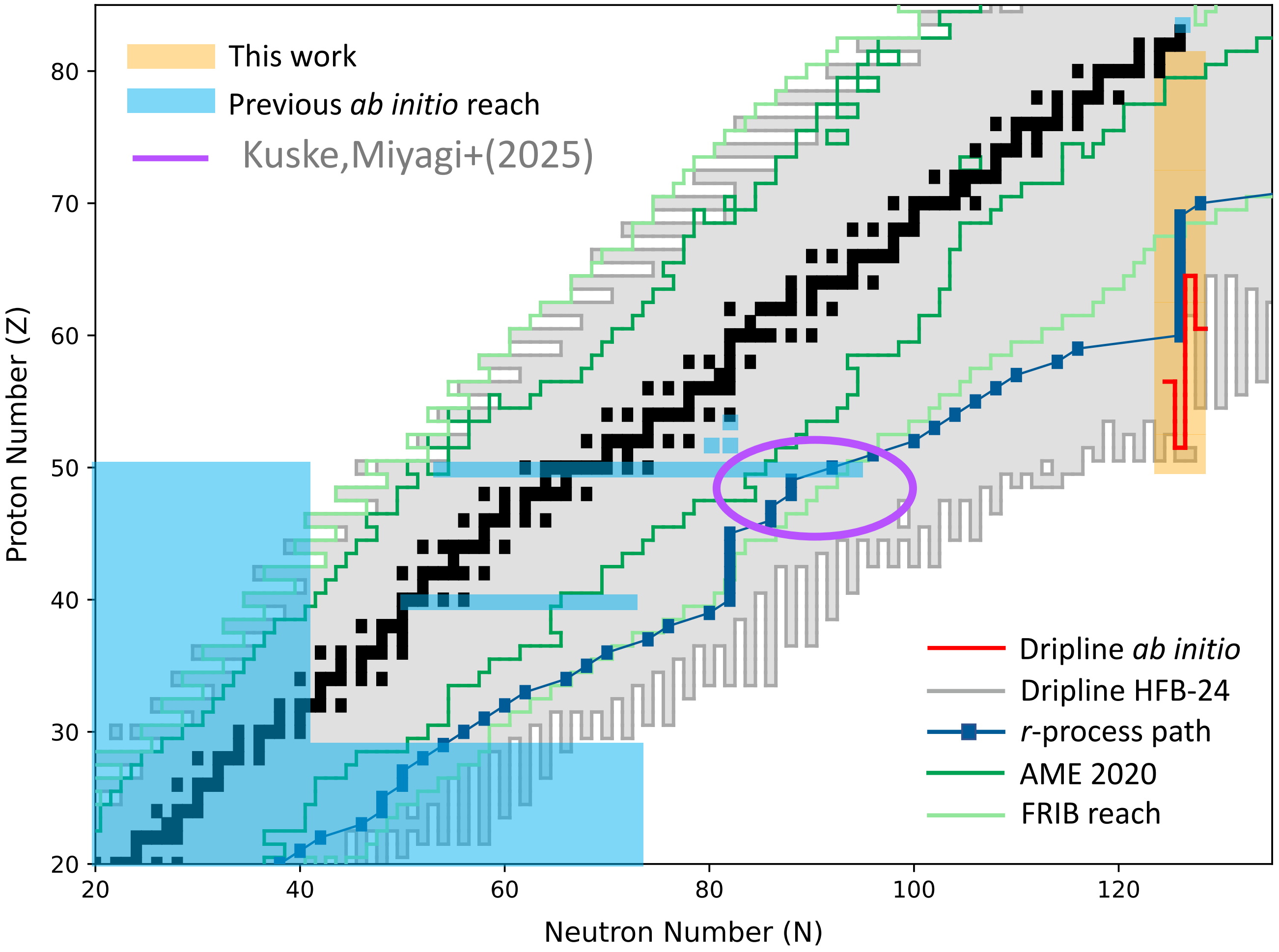

Hu, Larivière, Vassh, and Holt (in prep)

Ab initio nuclear theory: new reach into *r*-process nuclei

New *ab initio* masses change predictions for key heavies like Os, Ir, Pt in NSM nucleosynthesis calculations, adjusting what may have been concluded about Solar and stellar enrichment sources

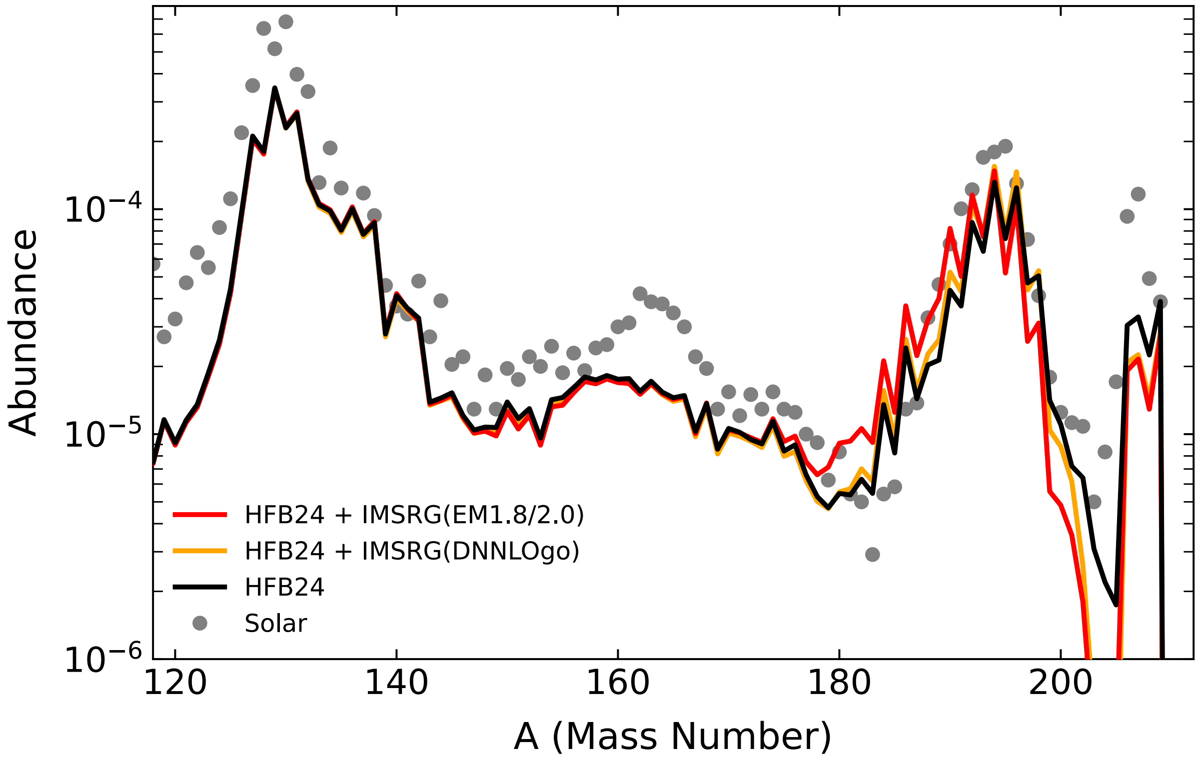

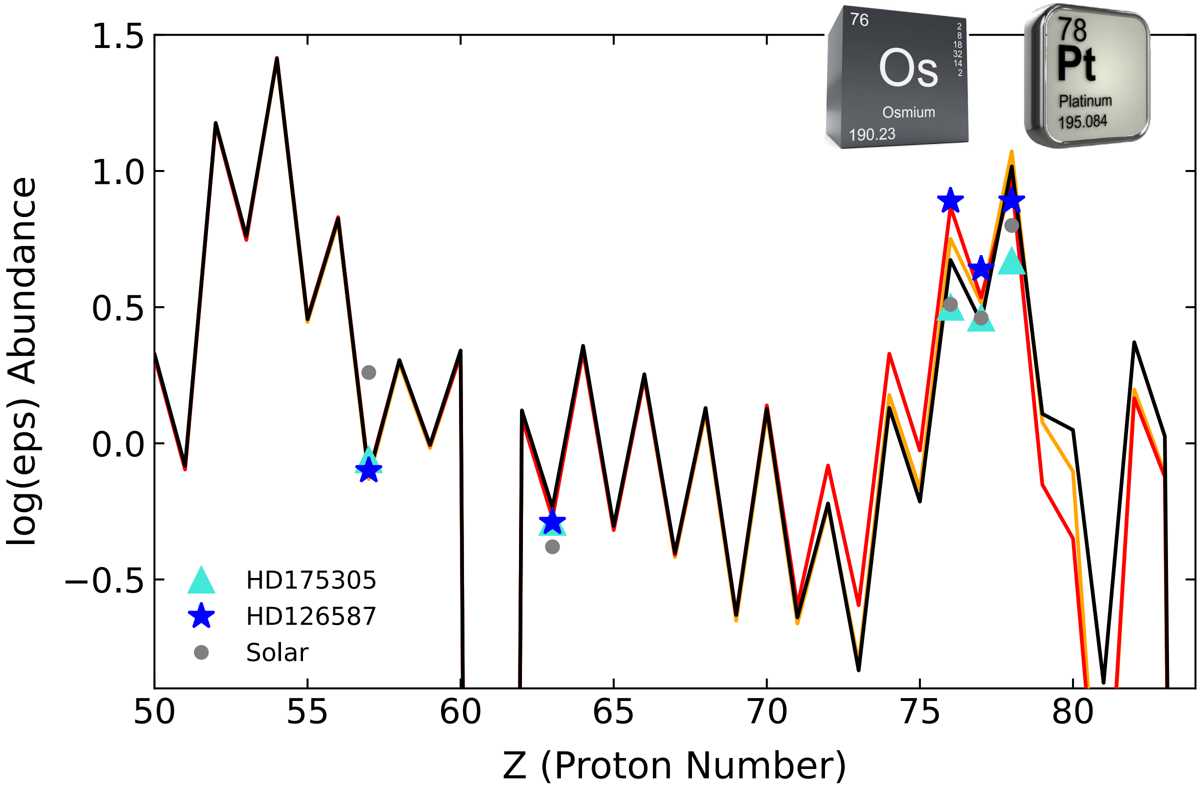

Hu, Larivière, Vassh, and Holt (in prep)

Towards refining calculations of *r*-process observables → **Interdisciplinary science and integrated approaches are key**

Solar system abundances as observed in meteorites

Metal-poor star abundances

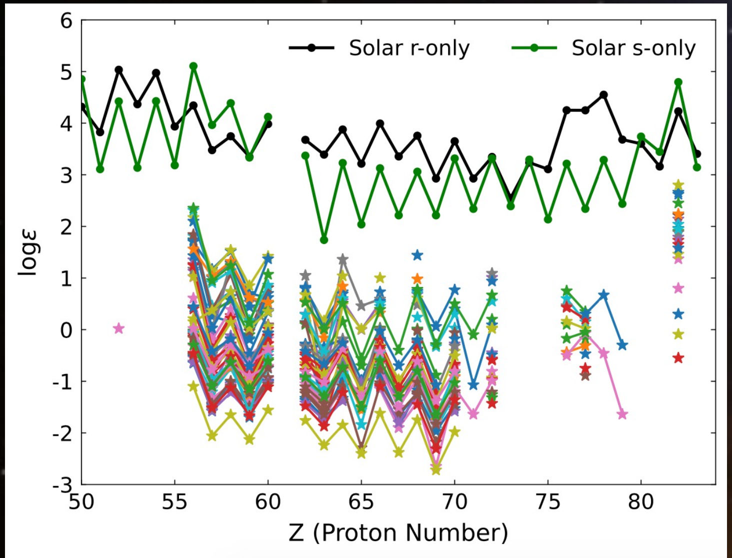

EM emission from rare events

Telescope Campaigns

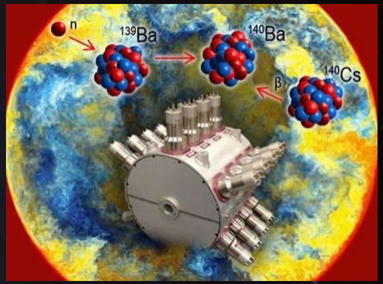

Nuclear Experiment

Machine Learning

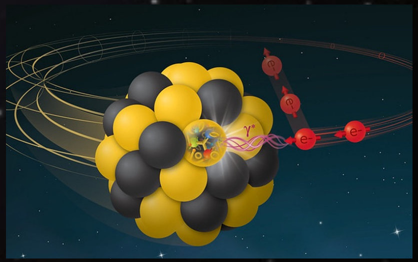

Nuclear Theory